Tectonics, hydrothermalism, and paleoclimate recorded by Quaternary travertines and their spatio-temporal distribution in the Albegna basin, central Italy: Insights on Tyrrhenian margin neotectonics

Gianluca Vignaroli[1,2,*], Gabriele Berardi[2], Andrea Billi[1], Sándor Kele[3], Federico Rossetti[2], Michele Soligo[2], and Stefano M. Bernasconi[4]

[1]CONSIGLIO NAZIONALE DELLE RICERCHE (CNR), ISTITUTO DI GEOLOGIA AMBIENTALE E GEOINGEGNERIA, AREA DELLA RICERCA DI ROMA 1, VIA SALARIA KM 29, 300–00015, MONTEROTONDO STAZIONE, ROME, ITALY

[2]DIPARTIMENTO DI SCIENZE, SEZIONE DI GEOLOGIA, UNIVERSITÀ DEGLI STUDI DI ROMA TRE, 00146 ROME, ITALY

[3]HUNGARIAN ACADEMY OF SCIENCES, RESEARCH CENTRE FOR ASTRONOMY AND EARTH SCIENCES, INSTITUTE FOR GEOLOGICAL AND GEOCHEMICAL RESEARCH, H-1112 BUDAPEST, HUNGARY

[4]ETH ZÜRICH, GEOLOGICAL INSTITUTE, 8092 ZÜRICH, SWITZERLAND

ABSTRACT

The Neogene–Quaternary Albegna basin (southern Tuscany, central Italy), located to the south of the active geothermal field of Monte Amiata, hosts fossil and active thermogene travertine deposits, which are used in this study to reconstruct the spatio-temporal evolution of the feeding hydrothermal system. Travertine deposition is controlled by regional tectonics that operated through distributed N-S– and approximately E-W–striking transtensional fault arrays. The geochronological data set ($^{230}Th/^{234}U$, uranium-series disequilibrium) indicates a general rejuvenation (from >350 to <40 ka) of the travertine deposits moving from north to south and from higher to lower elevations. Negative $\delta^{13}C$ and positive $\delta^{18}O$ trends with younger deposition ages and lower depositional elevations provide evidence for a change in space and time of the hydrothermal fluid supply, suggesting a progressive dilution of the endogenic fluid sources by increasing meteoric water inputs. Comparison with paleoclimate records suggests increased travertine deposition during humid interglacial periods characterized by highstands of the water table. Travertine deposits of the Albegna basin record the interactions and feedbacks among tectonics, hydrothermalism, and paleoclimate within a region of positive geothermal anomaly during the Quaternary. Our study also sheds light on the neotectonic evolution of the Tyrrhenian margin of central Italy, where hydrothermalism has been distributed along margin-transverse structures during the Pleistocene and Holocene. It is hypothesized that originally upper-crustal, margin-transverse faults have evolved to through-going crustal features during the Quaternary, providing structurally controlled pathways for hydrothermal fluids. We suggest that this was the consequence of a change in the relative magnitude of the principal stress vectors along the Tyrrhenian margin that occurred under a regional stress field dominated by a continuous extensional regime.

LITHOSPHERE; v. 8; no. 4; p. 335–358; GSA Data Repository Item 2016147 | Published online 20 May 2016 doi:10.1130/L507.1

INTRODUCTION

Hydrothermal settings are common in many tectonically active continental regions (Browne, 1978; Bibby et al., 1995; Rae et al., 2003; Newell et al., 2005; Crossey et al., 2006; Uysal et al., 2009; Cas et al., 2011; Mazzini et al., 2012; Baillieux et al., 2013; Karlstrom et al., 2013; Ricketts et al., 2014; Sella et al., 2014), where active faulting and fracturing provide viable pathways for circulation and mixing of endogenic and meteoric fluids, leading to diffuse mineralization and hydrothermal outflow (Curewitz and Karson, 1997; Cox et al., 2001; Rowland and Sibson, 2004; Billi et al., 2007; Gudmundsson, 2011; Bigi et al., 2014; Crossey et al., 2015; Vignaroli et al., 2015).

In hydrothermal settings where carbonate-enriched fluids circulate within calcareous reservoirs, thermogene travertine is the common $CaCO_3$ sinter precipitated from thermal springs (Pentecost and Viles, 1994; Pentecost, 1995). Thermogene travertine deposits have been documented to represent important markers for the mode and style of tectonic activity within hydrothermal settings (e.g., Altunel and Hancock, 1993; Hancock et al., 1999; Altunel and Karabacak, 2005; Uysal et al., 2007; Faccenna et al., 2008; Brogi and Capezzuoli, 2009; Brogi et al., 2010a; De Filippis and Billi, 2012; De Filippis et al., 2013b; Frery et al., 2015). Moreover, thermogene travertine has been used as a reliable indicator of paleoclimatic oscillations (Sturchio et al., 1994; Rihs et al., 2000; Soligo et al., 2002; Faccenna et al., 2008; Uysal et al., 2009; De Filippis et al., 2013a; Toker et al., 2015) and paleohydrological regimes (Crossey et al., 2006; Crossey and Karlstrom, 2012; Priewisch et al., 2014).

The region of Tuscany in central Italy (Fig. 1) is characterized by diffuse fossil and active hydrothermalism associated with highly productive geothermal areas of the Larderello-Travale and Mount Amiata fields (Batini et al., 2003). These geothermal fields are characterized by heat flux higher than 600 mW·m^{-2} (Della Vedova et al., 2001) and collectively provide an annual electrical production of more than 5300 GWh (Bertani, 2005). Hydrothermalism in Tuscany is originated by high heat flow due to Miocene–Quaternary postorogenic thinning of the central Apennines chain (present-day crustal thickness is ~22–24 km; Locardi and Nicolich, 1988; Billi et al., 2006) and associated emplacement of dominantly anatectic products of the late Miocene–Pleistocene Tuscan magmatic province (Innocenti et al., 1992; Marinelli et al., 1993; Serri et al., 1993;

*Corresponding author: gianluca.vignaroli@igag.cnr.it

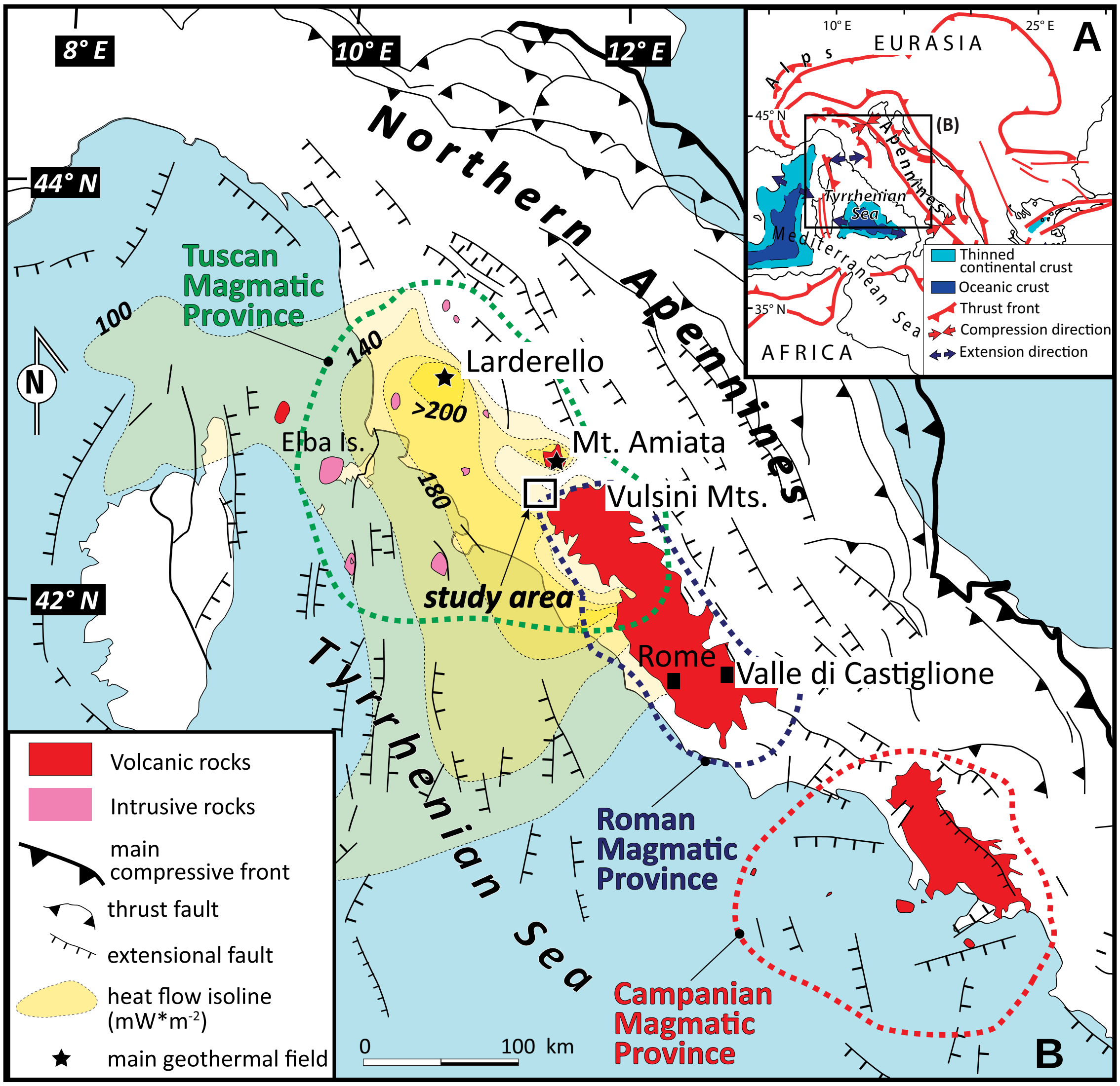

Figure 1. (A) Schematic tectonic map of the central Mediterranean region illustrating the trend of the main thrust fronts and the location of back-arc extensional domains (modified after Jolivet et al., 1998). (B) Geological map of the Northern Apennines (Italy) showing main extensional fault systems, magmatic provinces (Tuscan magmatic province and Roman magmatic province; after Peccerillo, 2003; Buttinelli et al., 2014), heat-flow isolines (after Della Vedova et al., 2001), and geothermal fields. The study area near the Mount Amiata and Vulsini Mountains volcanic districts is also shown.

Carmignani et al., 1994; Jolivet et al., 1998). Active hydrothermal springs and gas manifestations, including active travertine-depositing springs (e.g., Minissale, 2004; Barazzuoli et al., 2013; Capezzuoli, 2013), are the main present-day features of ongoing hydrothermal activity, particularly in southern Tuscany (Figs. 1 and 2). Recent studies of travertine and hydrothermal ore deposits have documented structurally controlled fluid flow in the region (e.g., Bellani et al., 2004; Brogi and Fabbrini, 2009; Brogi et al., 2010a; Liotta et al., 2010; Rossetti et al., 2007, 2011; Rimondi et al., 2015; Croci et al., 2016; Berardi et al., 2016). In particular, Pliocene–Pleistocene faulting has played a primary role in the endogenic fluid circulation that fed and still feeds some geothermal fields and $CaCO_3$-rich springs in the Mount Amiata geothermal area (Brogi et al., 2012). This geological setting makes Tuscany an excellent area for studying the relationships between hydrothermalism and tectonics, and their spatio-temporal evolution, through thermogene travertine deposits.

This paper addresses the relationships among Quaternary hydrothermalism, tectonics, and paleoclimatic evolution in the Neogene–Quaternary Albegna basin of southern Tuscany (Fig. 2). Our multidisciplinary approach integrates structural investigations, geochronological analyses ($^{230}Th/^{234}U$, uranium-series disequilibrium), and stable isotope ($\delta^{13}C$ and $\delta^{18}O$) systematics on selected carbonate structures (bedded and banded travertines and calcite-filled veins). The main objectives are (1) to reconstruct the spatio-temporal evolution of a hydrothermal system in a tectonically controlled area of geothermal interest, and (2) to discuss possible implications for the neotectonic regime along the Tyrrhenian margin in central Italy.

GEOLOGICAL SETTING

Southern Tuscany is part of the hinterland domain (on the Tyrrhenian Sea) of the Paleogene–Quaternary Northern Apennines chain (Fig. 1), a

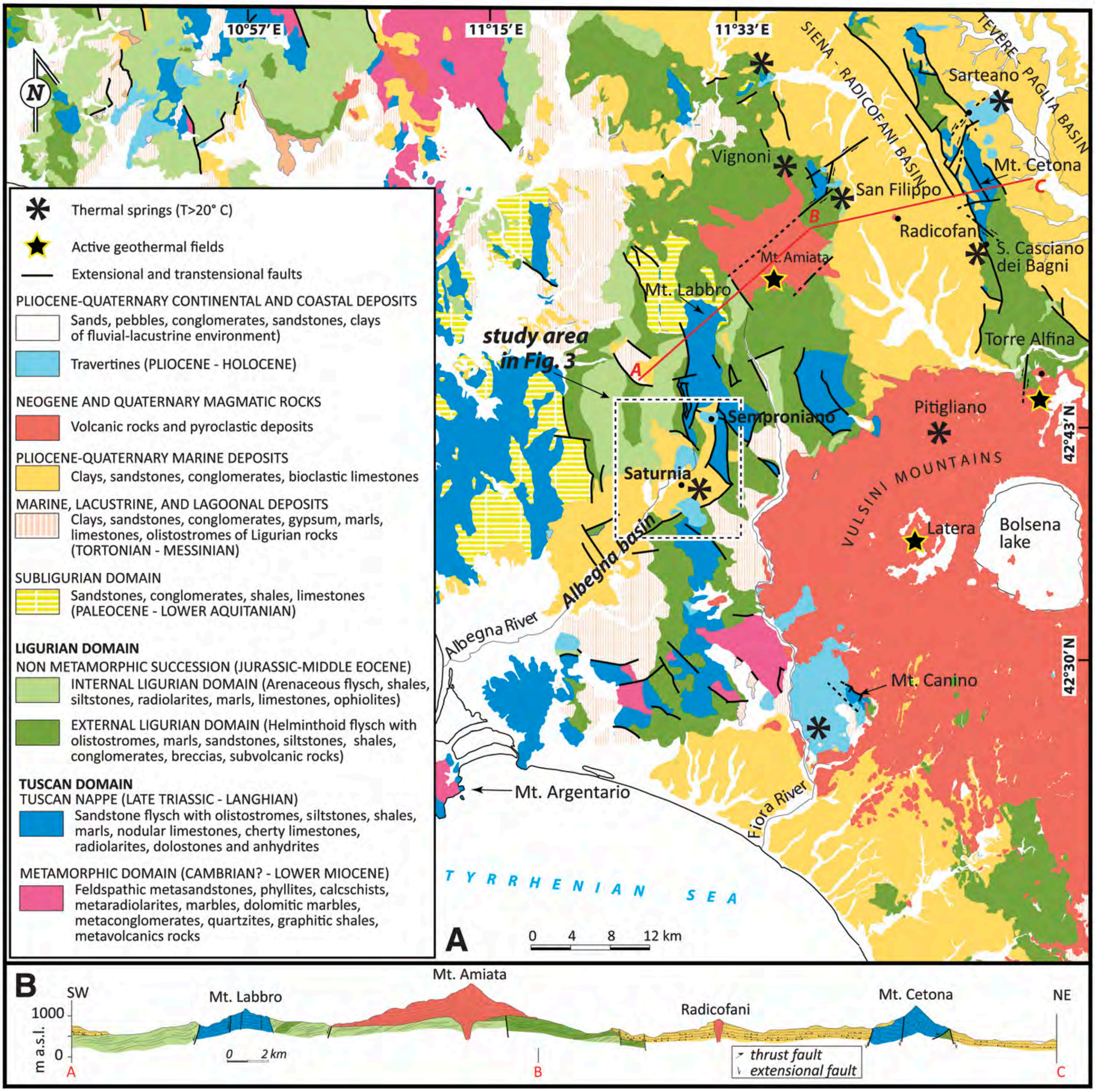

Figure 2. (A) Geological-structural map of southern Tuscany showing main postorogenic fault zones and travertine deposits (partially redrawn and adapted after Carmignani et al., 2013). The location of the study area is indicated with a dashed rectangle. Tectonic structures are from Costantini et al. (1984), Buonasorte et al. (1988), Martelli et al. (1989), Brogi (2008), Brogi et al. (2010, 2012), Carmignani et al. (2013), and Vignaroli et al. (2013). The map also shows main geothermal fields and thermal springs (after Minissale, 2004). (B) Geological cross section through the Mount Amiata volcanic district (redrawn and adapted after Jacobacci et al., 1967) showing postorogenic structures such as faults, sedimentary basins, and volcanic districts. See the A-B-C cross-section track in A.

fold-and-thrust belt resulting from Mesozoic–Cenozoic tectonic convergence between the European and African plates (e.g., Dewey et al., 1989; Boccaletti et al., 1990; Wortel and Spakman, 2000). Orogenic construction of the Apennines occurred simultaneously with the westward subduction of oceanic lithosphere and progressive involvement of the Adriatic (African affinity) continental margin (Royden et al., 1987; Doglioni, 1991; Faccenna et al., 2004; Rosenbaum and Lister, 2004). The growth of the Apennines involved a general eastward migration of thrust fronts and foredeep basins in a classical piggyback sequence toward the foreland (e.g., Patacca et al., 1990; Cipollari and Cosentino, 1995; Massoli et al., 2006). Since Miocene time, a postorogenic extensional regime has occurred in the hinterland (Tyrrhenian side) domain of the Apennines, producing crustal-scale extensional fault systems, which have dissected the thick orogenic pile (e.g., Malinverno and Ryan, 1986; Jolivet et al., 1998; Cavinato and DeCelles, 1999).

In southern Tuscany (Fig. 2A), Miocene-to-Quaternary postorogenic sedimentary sequences (Martini and Sagri, 1993; Liotta, 1994; Pascucci et al., 2006; Brogi and Liotta, 2008; Brogi, 2011; Brogi et al., 2013, 2014) unconformably overlie a tectonic nappe stack composed of, from top to bottom (Carmignani et al., 2013, and references therein): (1) oceanic-derived units of the Ligurian domain, consisting of marly-arenaceous flysch-type and discontinuous ophiolitic sequences (Lower Cretaceous to Upper Eocene in age), and (2) continental-derived units of the Tuscan domain, including a nonmetamorphic succession (Mesozoic carbonate and Cenozoic marly and siliciclastic sedimentary sequences of the Tuscan nappe) and underlying metamorphic units of the Tuscan metamorphic domain. These units are presently exposed in NNW-SSE–trending (as in the Mount Cetona area) and N-S–trending (as in the Mount Labbro area) elongate structural highs bounded by extensional and transtensional faults (e.g., Brogi, 2004a; Bonciani et al., 2005; Brogi and Fabbrini, 2009; Carmignani et al., 2013; Fig. 2B).

There are two opposing interpretations of the Neogene–Quaternary tectonics of southern Tuscany. The most common interpretation favors a postorogenic extensional regime acting at the rear (west) of the eastward-migrating compressional front (e.g., Carmignani et al., 1994; Keller et al., 1994; Lavecchia et al., 1994; Faccenna et al., 1997; Barchi et al., 1998; Jolivet et al., 1998; Martini et al., 2001; Collettini et al., 2006). This regime has led to the formation of orogen-parallel extensional basins, where NW-striking basin-boundary faults have been dissected by transverse transfer zones, the latter accommodating differential rates and amounts of extension between adjacent extensional compartments (Liotta, 1991; Faccenna et al., 1994; Acocella and Funiciello, 2002, 2006; Liotta et al., 2015). Alternatively, a Miocene–Pliocene shortening regime has been described as having been active in Tuscany, causing basement duplexing and out-of-sequence thrusting (e.g., Boccaletti et al., 1997; Cerrina Feroni et al., 2006; Musumeci and Vaselli, 2012; Bonini et al., 2014). In this latter interpretation, extensional and strike-slip faulting would represent the most recent mode of deformation in Tuscany.

Late Miocene–Quaternary magmatism is localized along the Tyrrhenian margin (Fig. 1; e.g., Peccerillo, 2003; Conticelli et al., 2015) and characterized in Tuscany by acidic intrusive and volcanic products with associated high-temperature metamorphism (e.g., Barberi et al., 1971; Innocenti et al., 1992; Serri et al., 1993; Acocella and Rossetti, 2002; Rocchi et al., 2002; Dini et al., 2005; Rossetti et al., 2007, 2008; Farina et al., 2010; Cifelli et al., 2012). The Tuscan magmatic province hosts fossil and active hydrothermal systems. Endogenic fluid circulation within hydrothermal systems has been dominantly channelized by possibly active extensional faults (e.g., Barberi et al., 1994; Buonasorte et al., 1988; Chiarabba et al., 1995; Gianelli et al., 1997; Batini et al., 2003; Bellani et al., 2004; Annunziatellis et al., 2008; Brogi, 2008; Brogi et al., 2010b, 2015; Liotta et al., 2010; Rossetti et al., 2008, 2011).

The Mesozoic carbonate units of the Tuscan nappe have exerted a pivotal role in the functioning of the entire geothermal-hydrothermal setting of Tuscany. At surface and shallow levels, these rocks provide the recharge areas where meteoric waters infiltrate to depth thanks to the well-developed fault-fracture permeability network. At depth, carbonate rocks constitute the reservoirs where meteoric and endogenic fluids circulate and mix before ascending to feed surface thermal springs and CO_2 emission centers (e.g., Batini et al., 2003; Minissale, 2004). Active and fossil travertine deposits occur with variable size and shape in proximity to exposed Mesozoic carbonates and at the peripheries of main volcanic centers (Mount Amiata and Vulsini Mountains in Fig. 2A). As explained already, these travertine deposits originated from the long-term interactions among faults, fractures, and hydrothermal fluids during the Quaternary (Brogi, 2004b; Brogi et al., 2012).

The Albegna basin (Fig. 2A) is delimited to the north by the Mount Amiata volcanic district (300–190 ka; Cadoux and Pinti, 2009; Laurenzi et al., 2015; Marroni et al., 2015) and to the southeast by the Vulsini Mountains volcanic district (590–127 ka; Nappi et al., 1995). The Albegna basin is filled by marine and transitional sediments, which are late Miocene to Quaternary in age. These deposits consist of marine clays, regressive sands, gravels, and conglomerates covered by eolian sands and fluvial clays (Zanchi and Tozzi, 1987; Bettelli et al., 1990; Bonazzi et al., 1992; Bossio et al., 1993, 2003). Steeply-dipping, N-S–, E-W–, and NE-SW–striking tectonic structures, mainly consisting of extensional and oblique to strike-slip faults, dissect the basin-filling deposits (Fig. 3A; Zanchi and Tozzi, 1987; Brogi, 2004a; Bellani et al., 2004; Brogi and Fabbrini, 2009). Both extensional and strike-slip fault systems disarticulated the substratum, exposing the Jurassic units to the north of the study area (Fig. 3B; e.g., Bettelli et al., 1990; Brogi, 2004a; Bonciani et al., 2005; Carmignani et al., 2013; Guastaldi et al., 2014).

Both regional uplift (related both to regional tectonics and to the Mount Amiata volcanic bulging) and eustatic fluctuations contributed to the morphological shaping of the Albegna basin during the Pleistocene–Holocene period (Piccini et al., 2015). In fact, marine Pliocene sediments presently occur up to ~600 m above sea level (a.s.l.), and multiple Quaternary alluvial terraces occur at different elevations between 50 and 300 m a.s.l. The present landscape of low rolling hills is dominated by the alternation of morphological depressions (mostly filled by Quaternary deposits) and positive morphotypes, both being affected by well-pronounced escarpments and canyon incisions.

As demonstrated by the geochemistry of numerous thermal springs, the hydrogeological setting of the Albegna basin and surrounding areas is mainly conditioned by the deep aquifer occurring within the Mesozoic carbonate units of the Tuscan nappe (e.g., Baldi et al., 1973; Duchi et al., 1992; Chiodini et al., 1995; Minissale, 2004). This aquifer has experienced significant vertical oscillations during the Quaternary, as also shown by the occurrence of speleogenic markers and landscape changes (Piccini et al., 2015). Presently, the general southward drainage is toward the Saturnia thermal springs (Fig. 2A), where gas emissions and travertine deposition are still active (Minissale, 2004).

In the northern part of the Albegna basin, a series of travertine deposits lies unconformably on top of the Neogene sediments (Zanchi and Tozzi, 1987; Bosi et al., 1996; Barilaro et al., 2012). Some of these travertine deposits are affected by faults with associated damage zones and joint networks. These deformations have been considered as resulting from either Pliocene–Pleistocene extensional tectonics (Zanchi and Tozzi, 1987), or alternating contractional and extensional tectonic phases active in southern Tuscany during the late Pleistocene (Martelli et al., 1989). Based on morphological and stratigraphic characteristics of the Albegna travertine deposits, Bosi et al. (1996) proposed discrete phases of travertine deposition over a long time interval between Messinian and Holocene times. So

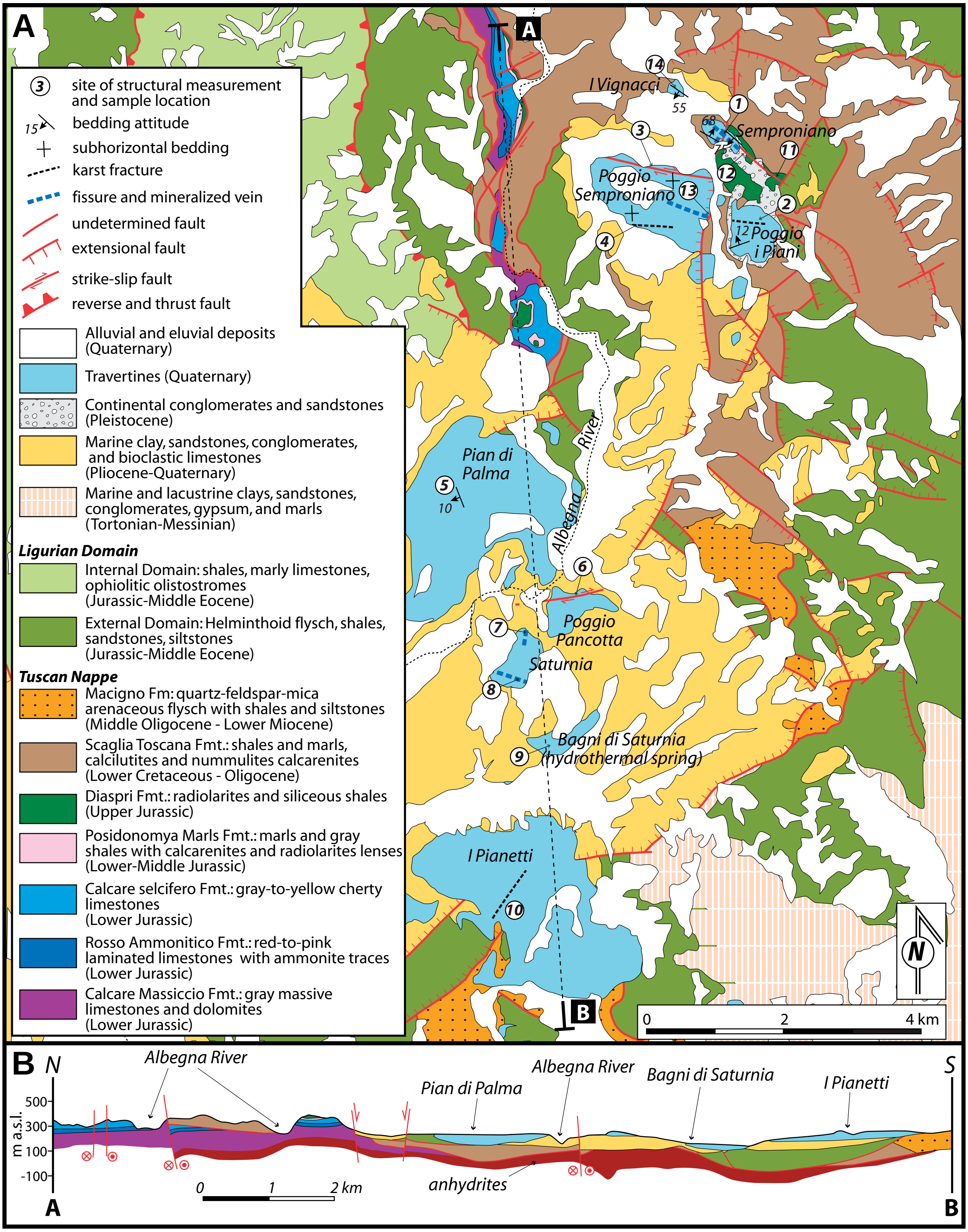

Figure 3. (A) Structural map of the study area with structural measurement sites shown with numbers within circles (see Table 1). The map is based on the geological map at the 1:10,000 scale available online at http://www.regione.toscana.it/-/geologia. (B) N-S geological cross section (redrawn and adapted after Guastaldi et al., 2014) illustrating the geometric-structural relationships between the studied travertine deposits and the underlying units.

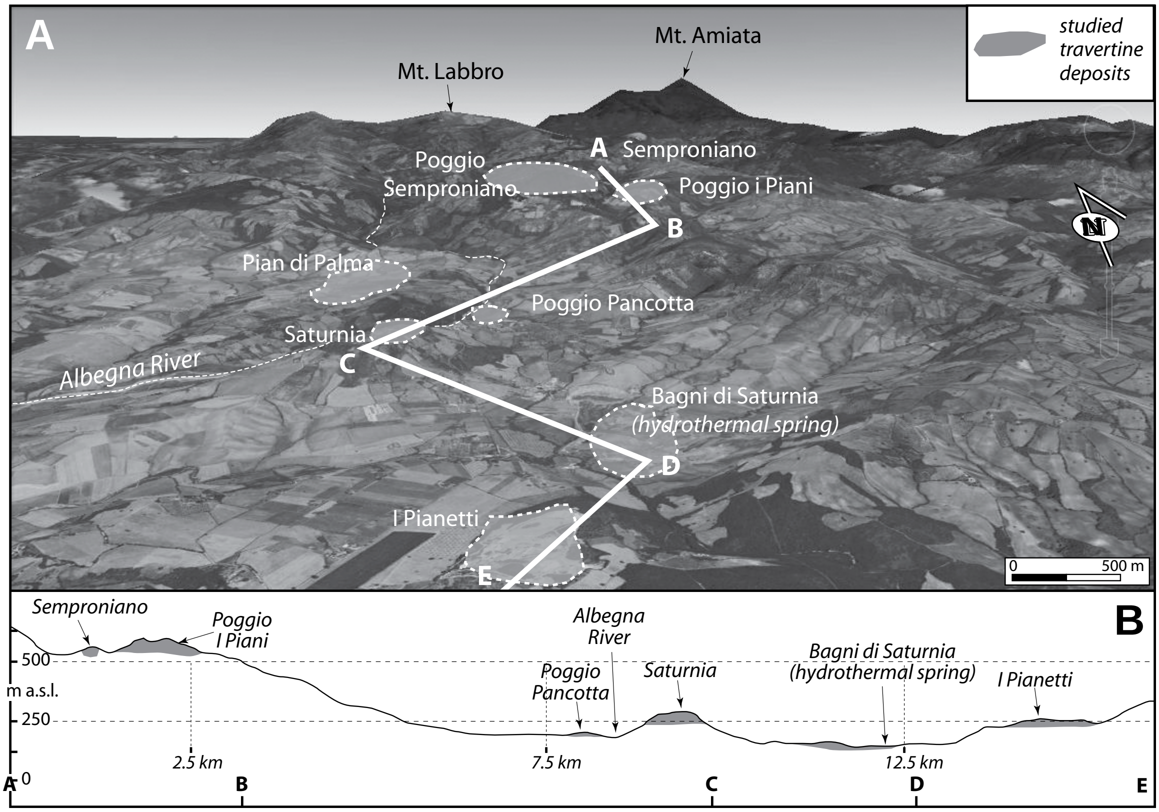

Figure 4. (A) Northward panoramic view (Google Earth image) with locations of the studied travertine deposits in the Albegna basin. (B) Topographic profile illustrating the elevation of the main travertine deposits. The travertine elevation decreases from north (Semproniano) to south (Saturnia), where hydrothermal manifestations and thermogene travertine deposition are active. See the A-B-C-D-E profile track in A.

far, the only available radiometric age (218 +39/–27 ka) for the Albegna travertine deposits was determined on a travertine sample collected in a quarry located immediately to south of the village of Saturnia (Taddeucci and Voltaggio, 1987). Additional radiometric dating is thus required to constrain (1) the ages of these travertine deposits and (2) their possible relationships with the hydrothermal, tectonic, and climatic conditions within the Albegna basin and the greater Tuscan region.

WORKFLOW, METHODS, AND NOMENCLATURE

Structural investigations were carried out along a N-S–trending transect in the northern part of the Albegna basin, where series of travertine deposits are exposed. From north to south, these deposits are named: Semproniano Ridge, Poggio Semproniano, Poggio i Piani, Pian di Palma, Poggio Pancotta, Saturnia village, Bagni di Saturnia, and I Pianetti (Fig. 4A; Table 1). Field observations were focused on the recognition of: (1) the different travertine morphotypes (plateau vs. fissure ridge travertines), (2) the different styles of travertine deposition and precipitation (bedded vs. banded travertines), (3) the geometric relationships between the travertine deposits and the surrounding units, and (4) the structural features (fault and fracture systems) postdating travertine deposition. Fault and fracture systems were studied in terms of their geometry (attitude, spacing, aperture, persistence, and crosscutting relationships) and kinematics. Results of our field investigations (Table 2) are synthesized in the geological-structural map of Figure 3A.

Fissure ridges are defined as elongate mound-shaped travertine deposits, straight or curved in map view, with a main crestal fissure, and length spanning from a few meters to several hundreds of meters (e.g., Hancock et al., 1999; Altunel and Karabacak, 2005; Brogi and Capezzuoli, 2009; De Filippis and Billi, 2012; De Filippis et al., 2013b). Travertine plateaus are defined as travertine deposits characterized by centimeter-thick, subhorizontal bedding. Travertine plateaus are tabular bodies roughly equidimensional in map view, often resulting in topographic highs.

Bedded travertines are the primary travertine strata formed during open-air $CaCO_3$ precipitation from saturated H_2O solutions. Banded travertine are the $CaCO_3$ precipitates filling fractures that cut through the bedded travertines (and also other host rocks) or develop in a sill-like fashion along the travertine beds themselves. These structures are usually filled by sparitic and variably colored bands of $CaCO_3$ precipitated in a non-open-air (intralithic) environment (e.g., Uysal et al., 2007; De Filippis et al., 2013a). We use the term veins only for fractures filled by nonbanded sparry calcite with maximum thicknesses of a few centimeters.

Bedded and banded travertines, veins, and speleothem-like concretions were systematically sampled across the study area for geochronological and isotopic analyses. Samples were dated using the $^{230}Th/^{234}U$ method (Ivanovich and Harmon, 1992), which is based on the fractionation of the parent isotopes ^{238}U and ^{234}U from their long-lived daughter ^{230}Th. This technique assumes that thorium is not included in the crystal lattice of the carbonate at the time of deposition, being easily hydrolyzed and precipitated or adsorbed on the detrital fraction, whereas uranium is

TABLE 1. MAIN CHARACTERISTICS OF THE TRAVERTINE DEPOSITS IN THE ALBEGNA BASIN

Travertine deposit	Latitude	Longitude	Elevation (m a.s.l.)	Estimated thickness (m)	Travertine morphotype	Travertine type
Semproniano village	42°43′51″N	11°32′25″E	550–590	50 (?)	Fissure ridge	Banded
Poggio Sempronaniano	42°43′25″N	11°31′46″E	500–700	200	Plateau, positive morphostructure	Bedded
Poggio I Piani	42°43′19″N	11°32′38″E	580–630	50	Plateau, positive morphostructure	Bedded
Pian di Palma	42°41′21″N	11°29′58″E	220–230	20 (?)	Plateau, depressed morphostructure	Bedded
Poggio Pancotta	42°40′28″N	11°30′42″E	195–215	20	Plateau, positive morphostructure	Bedded
Saturnia village	42°39′51″N	11°30′14″E	250–290	40	Plateau, positive morphostructure	Bedded with local banded
Bagni di Saturnia	42°38′53″N	11°30′43″E	142		Depressed morphostructure	Bedded
I Pianetti	42°38′01″N	11°30′34″E	220–260	40	Plateau, depressed morphostructure	Bedded with intrusive veins

TABLE 2. SUMMARY OF THE MAIN STRUCTURAL FEATURES OBSERVED DURING THE FIELD SURVEY

Structural measurement site	Latitude	Longitude	Location	Lithology	Structures	Figure
1	42°43′51″N	11°32′25″E	Sempronaniano village	Travertine	Fissure ridge, banded travertine, secondary fracture and N-S faulting	Figs. 5 and 8
2	42°43′25″N	11°31′46″E	Poggio i Piani	Travertine	Bedding, karst-fracture network	Fig. 6, Fig. DR1*
3	42°43′32″N	11°31′52″E	Poggio Sempronaniano (northern side)	Travertine	Bedding, E-W–striking dextral strike-slip fault zone	Figs. 6 and 7
4	42°43′13″N	11°31′42″E	Poggio Sempronaniano (southern side)	Travertine	Bedding, karst-fracture network	Fig. 6
5	42°41′21″N	11°29′58″E	Pian di Palma	Travertine	Bedding, subhorizontal karst cavities	Fig. 6
6	42°40′28″N	11°30′42″E	Poggio Pancotta	Travertine	ENE-WSE–striking dextral strike-slip fault zone	Fig. 7
7	42°40′18″N	11°30′22″E	North of Saturnia village	Travertine	Bedded-banded relationships	Fig. DR1*
8	42°39′51″N	11°30′15″E	Saturnia village (Roman gate)	Travertine	Bedded-banded relationships	Fig. 10
9	42°38′53″N	11°30′43″E	Bagni di Saturnia	Travertine	Bedding, depositional facies	Fig. 6
10	42°38′01″N	11°30′34″E	I Pianetti	Travertine	Karst-fracture network, bedding	Fig. 9
11	42°43′29″N	11°32′58″E	SE of Sempronaniano (abandoned quarry)	Diaspri Formation (Tuscan nappe)	NW-SE–striking strike-slip fault zone, bedding	Fig. DR1*
12	42°43′32″N	11°32′46″E	SE of Sempronaniano (public road)	Pleistocene continental deposits	NW-SE–striking strike-slip fault zone, bedding	Fig. DR1*
13	42°43′09″N	11°32′18″E	Poggio Sempronaniano (eastern side)	Scaglia Toscana Formation (Tuscan nappe) and travertine	Calcite-filled veins, bedding	Fig. 9
14	42°44′14″N	11°32′07″E	I Vignacci	Travertine	Fissure ridge, banded travertine	Fig. DR1*

*See text footnote 1.

soluble in the surface and near-surface environments, coprecipitating with $CaCO_3$ upon exsolution of CO_2. A $^{230}Th/^{234}U$ ratio close to one indicates that ^{230}Th and ^{234}U have reached secular equilibrium and therefore give an age older than the ca. 350 ka limit of the $^{230}Th/^{234}U$ dating method. The $^{13}C/^{12}C$ ($\delta^{13}C$) and the $^{18}O/^{16}O$ ($\delta^{18}O$) ratios of samples were investigated to distinguish between thermogene and meteogene carbonates and to characterize the origin and properties of the parental fluids (Friedman, 1970; Manfra et al., 1974; Fouke et al., 2000; Pentecost, 2005; Kele et al., 2011). In thermogene travertines, CO_2 mainly derives from deep magmatic fluids and from their interaction with carbonate rocks. Conversely, CO_2 in meteogene travertines mainly derives from the atmosphere and from shallow deposits such as soils (Turi, 1986; Kele et al., 2003; Pentecost, 2005). These distinct CO_2 sources are reflected in the $\delta^{13}C$ values, with thermogene travertines being characterized by $\delta^{13}C$ values between −3‰ and +8‰ and meteogene travertines being characterized by average $\delta^{13}C$ values of −8.48‰ (Pentecost, 2005). Eventually, from the $\delta^{18}O$ values, we calculated the temperature of the travertine and vein parental fluids using the equation of Kele et al. (2015).

RESULTS

Travertine Types

Fossil and active travertine deposits of the Albegna basin are aligned roughly N-S along an ~18 km transect (Fig. 4A) and are exposed at different elevations (Fig. 4B). The northernmost travertine deposits are represented by the isolated fissure ridge forming the bedrock of the Sempronaniano village at ~550 m a.s.l. and two thick plateaus (Poggio Sempronaniano and Poggio i Piani) forming positive morphological structures at ~600–700 m a.s.l. Moving southward, an additional travertine deposit is exposed in a morphological depression in the Pian di Palma locality (~230 m a.s.l.) on the northwest side of the Albegna River. On the southeast side, two travertine deposits form tabular positive morphological features in Poggio Pancotta (~200 m a.s.l.) and Saturnia (250–290 m a.s.l.). The southernmost travertine deposit, which is exposed at I Pianetti (~230 m a.s.l.), forms a roughly tabular feature filling a morphological depression. Active hydrothermalism and travertine deposition occur at

~140 m a.s.l. at Bagni di Saturnia. In the study area, this is the travertine deposit with the lowest elevation.

Studied travertine deposits were analyzed in terms of their morphological characteristics to understand the travertine morphotypes and their associated internal fabrics. The following outline refers to the field sites of structural measurements shown in Figure 3A. The Semproniano travertine (site 1) consists of a NW-SE–striking fissure-ridge structure (Berardi et al., 2016) located 500 m to the north of the Poggio i Piani and Poggio Semproniano travertine plateaus (sites 2 and 4, respectively; Fig. 5A). The exposed ridge is ~700 m long in the NW-SE direction and 400 m wide in the perpendicular direction. In the northwestern part, the ridge is in contact with Lower Cretaceous–Oligocene shales and marls of the Scaglia Toscana Formation (Tuscan nappe) and Pliocene–Quaternary marine clays and sandstones (Fig. 5B). In the southeastern part, the ridge is in contact with Upper Jurassic radiolarites and siliceous shales (Diaspri Formation of the Tuscan nappe; see also Gelmini et al., 1967). The structural relationships between the travertine deposit and the surrounding units are not clear due to the Quaternary sedimentary cover and anthropic backfill. The internal fabric of the travertine fissure ridge in the Semproniano village consists of a wide (50 m at least), vertical to subvertical banded travertine (Figs. 5C and 5D) extensively exposed below the Aldobrandeschi Fortress. The banded travertine consists of alternating centimeter-thick white bands (with calcite crystals growing perpendicular to the wall) and gray-colored finer-grained bands. These bands are generally parallel to one another and strike parallel to the fissure ridge (average strike N315°), dipping subvertically N70° or N210° (Fig. 5D). In places, intersecting bands create V-shaped geometries (Fig. 5C). Poorly preserved remnants of subhorizontal bedded travertine are exposed on the distal part of the southwestern flank of the fissure ridge. This bedded travertine consists of plane-parallel brown-colored centimeter-thick beds (Fig. 5E). Unlike the banded travertine, which is characterized by nonporous sparry calcium carbonate, the bedded travertine is characterized by calcite shrubs, laminations, and millimeter-to-centimeter–sized cavities of both syndepositional and postdepositional (karst) origin (Fig. 5F). The contact between the banded and bedded travertines is not clearly visible.

About 1 km to the northwest of Semproniano, an isolated deposit of travertine is exposed in the I Vignacci locality (site 14). The internal fabric of this deposit consists of banded travertine with NW-SE–striking bands (Fig. DR1A[1]), dipping steeply (~55°) to the N240°, at high angle with respect to the adjacent subhorizontal Pliocene–Quaternary sequence. The orientation of this banded travertine is very similar to the one observed in Semproniano (average strike: N145°). This evidence suggests a structural and geometric continuity between the I Vignacci and Semproniano village banded travertines.

At Poggio Semproniano and Poggio i Piani, the travertine plateaus are subhorizontal (Figs. 5A and 6A) and lie on top of the Pliocene–Quaternary marine sequence or on the Scaglia Toscana Formation. They consist of plane-parallel (Fig. 6B), centimeter-thick beds of white-colored lime-mudstone with heterogeneous porosity due to the presence of microbialites and millimeter-to-centimeter–sized karst-dissolution cavities (Fig. 6C). Bedding is generally horizontal (Fig. 6C), although locally complicated by fault-related tilting (see following).

The Pian di Palma (site 5) and I Pianetti (site 10) deposits consist of subhorizontal travertine plateaus filling local depressions. The Pian di Palma plateau has a horseshoe-like shape of ~6 km^2 in areal extent. An ~20 m thickness of this travertine is exposed in an abandoned quarry at Pian di Palma (Fig. 6D). The quarry exposure is characterized by thick beds (average thickness between 20 and 50 cm) affected by numerous postdepositional features such as calcite veins, subhorizontal karst cavities, and vertical karst conduits. The stratigraphic-structural relationships between this travertine plateau and the adjacent units are not well exposed. The travertine is laterally in contact with (and probably lies on top of) the Pliocene–Quaternary marine sequence, the architecture of which is controlled by NW-SE–striking and N-S–striking extensional faults (Fig. 3A).

The travertine plateau at I Pianetti has a subcircular shape and a maximum thickness of ~30 m, and it is visible in a large active quarry. The travertine is characterized by decimeter-thick, plane-parallel beds showing locally complex convoluted geometries.

At Saturnia (sites 7 and 8) and Bagni di Saturnia (site 9), the travertine deposits lie on top of the Pliocene–Quaternary marine sediments and mainly consist of bedded travertine boundstone with homogeneous primary porosity and millimeter-to-centimeter–sized karst-dissolution cavities. At the active travertine site of Bagni di Saturnia, different depositional facies are distinguished, including cascades, pools, and terraced slopes (Figs. 6E and 6F).

Postdepositional Structures

We studied the postdepositional structures affecting the travertine deposits in order to understand their geometry, spatial distribution, and tectonic and/or hydrothermal significance.

Faults

Fault sets with average orientations of N280°/75° and N75°/75° crosscut the northern limits of the exposures at Poggio Semproniano (site 3) and Poggio Pancotta (site 6), respectively (Fig. 7). At Poggio Pancotta, these fault sets are composed of damage zones (e.g., Caine et al., 1996) a few meters thick at the most (Fig. 7A). Fault planes dip steeply (> 50°) toward the NW or SE. Most slickenlines and abrasive striations on fault planes (Figs. 7B and 7E) are characterized by a pitch smaller than 10° or greater than 170° (see the stereographic projection in Fig. 7A), providing evidence for strike-slip–dominated kinematics. At Poggio Semproniano, an ~3-m-thick damage zone (Figs. 7C and 7D) is characterized by 30-cm-spaced fault surfaces and NNW-SSE–striking synthetic shear fractures (Riedel shears). Fault surfaces dip steeply (up to 80°) toward the NNE, whereas Riedel shears are subvertical or dip steeply toward the ENE (see the stereographic projection in Fig. 7D). Slickenlines and abrasive striations on fault planes are characterized by a pitch smaller than 15° or greater than 165° (see the stereographic projection in Fig. 7D). Collectively, the analysis of kinematic indicators (e.g., Riedel shears, lunate-cuspate morphologies on the striated fault planes; Fig. 7E) indicates a right-lateral shear for these E-W–striking faults affecting travertine deposits on both sites. On the other hand, a N-S–striking (N180°/80°) fault crosscuts the fissure ridge at Semproniano village and the eastern edge of the plateau at Poggio Semproniano. At Semproniano village (site 1), this fault develops a 0.5-m-wide damage zone within the banded travertine (Fig. 8A). Slickenlines on the fault surfaces are very difficult to determine. Very close to this N-S–striking fault, centimeters-thick (average thickness: 7–10 cm), NNE-SSW–striking fractures filled by light-brown speleothem-like concretions cut through the banded travertine (Figs. 8B and 8C). Geometrical relationships between the fault surface and these speleothem-filled fractures (here interpreted as tension fractures) suggest an oblique shear for this fault. This N-S–striking fault is probably the northern culmination of the extensional fault system that marks the contact between the Pliocene–Quaternary sedimentary deposits and the Tuscan nappe units south of the village of Semproniano (Fig. 3A).

Faults affecting the host rocks of the travertine deposits are not well exposed in the study area. NW-SE–striking faults have been recognized

[1]GSA Data Repository Item 2016147, Figure DR1 (with exposure photographs) and color versions of Figures 5–10, is available at www.geosociety.org/pubs/ft2016.htm, or on request from editing@geosociety.org.

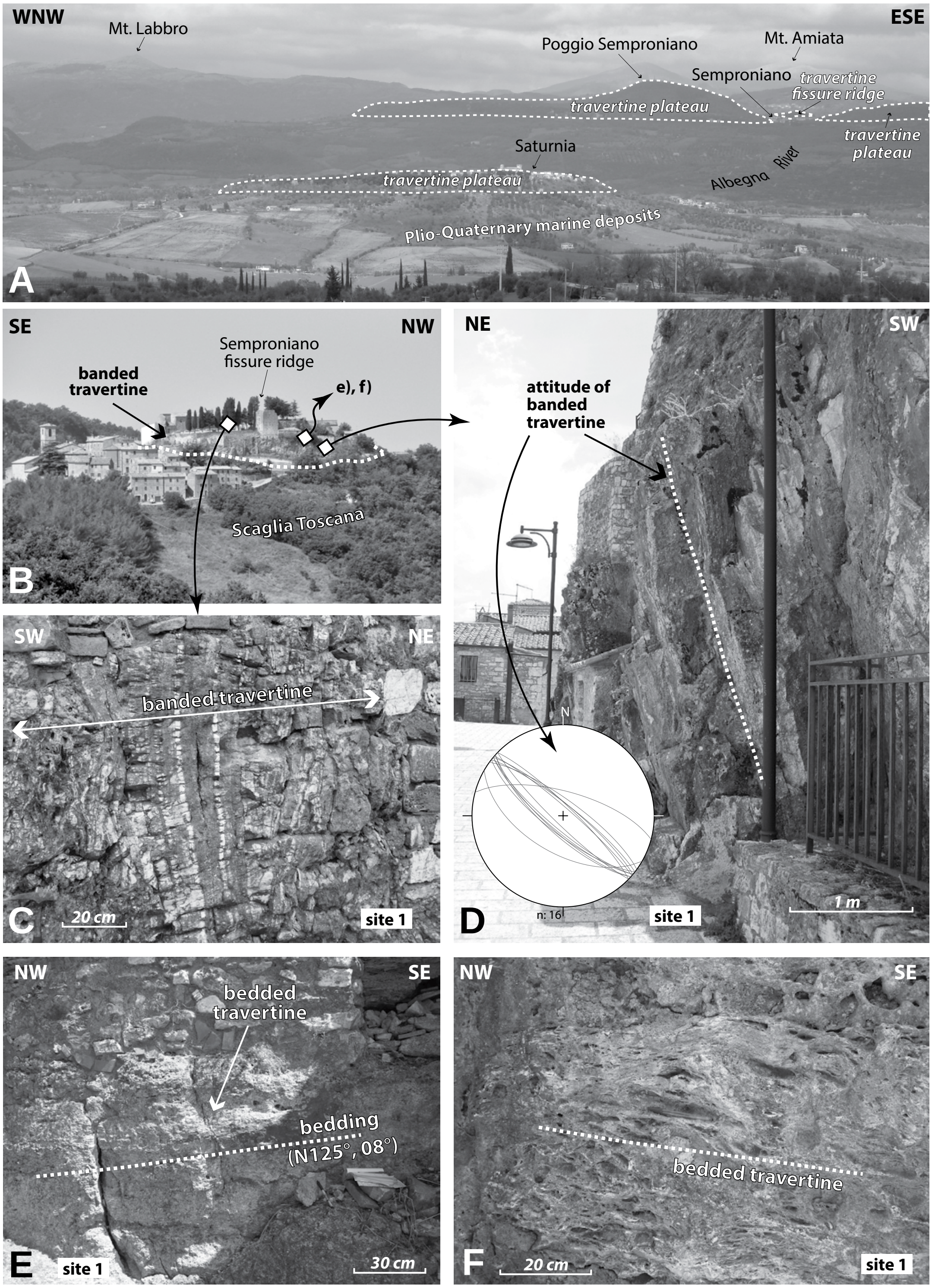

Figure 5. (A) Northeastward panoramic view of the study area showing the Mount Amiata volcanic district, the Mesozoic–Cenozoic carbonate reservoir exposed in the Mount Labbro area, and the studied travertine deposits. Travertine plateaus occur at Saturnia, Poggio Semproniano, and Poggio i Piani. The northernmost travertine deposit corresponds to the huge fissure ridge cropping out in the Semproniano village. (B) View of the fissure ridge travertine extensively exposed below the fortress of the Aldobrandeschi family (tenth century) in the Semproniano village. The host units are represented by the Pliocene deposits belonging to the postorogenic depositional cycle. (C) The central part of the fissure ridge (Semproniano) is characterized by a thick vein of banded travertine consisting of a rhythmic sequence of centimeter-thick crystallized levels of sparry calcite. (D) The banded travertine (Semproniano) is mainly oriented NW-SE and characterized by high dip values (see the stereoplot; stereographic projection, Schmidt net, lower hemisphere). (E) Subhorizontal, bedded travertine exposed in the southwestern flank of the fissure ridge (Semproniano). (F) Detail from the bedded travertine (Semproniano) with peculiar fabric defined by lamination, shrubs, and karst-dissolution cavities. Color version is available as part of the data repository item (see text footnote 1).

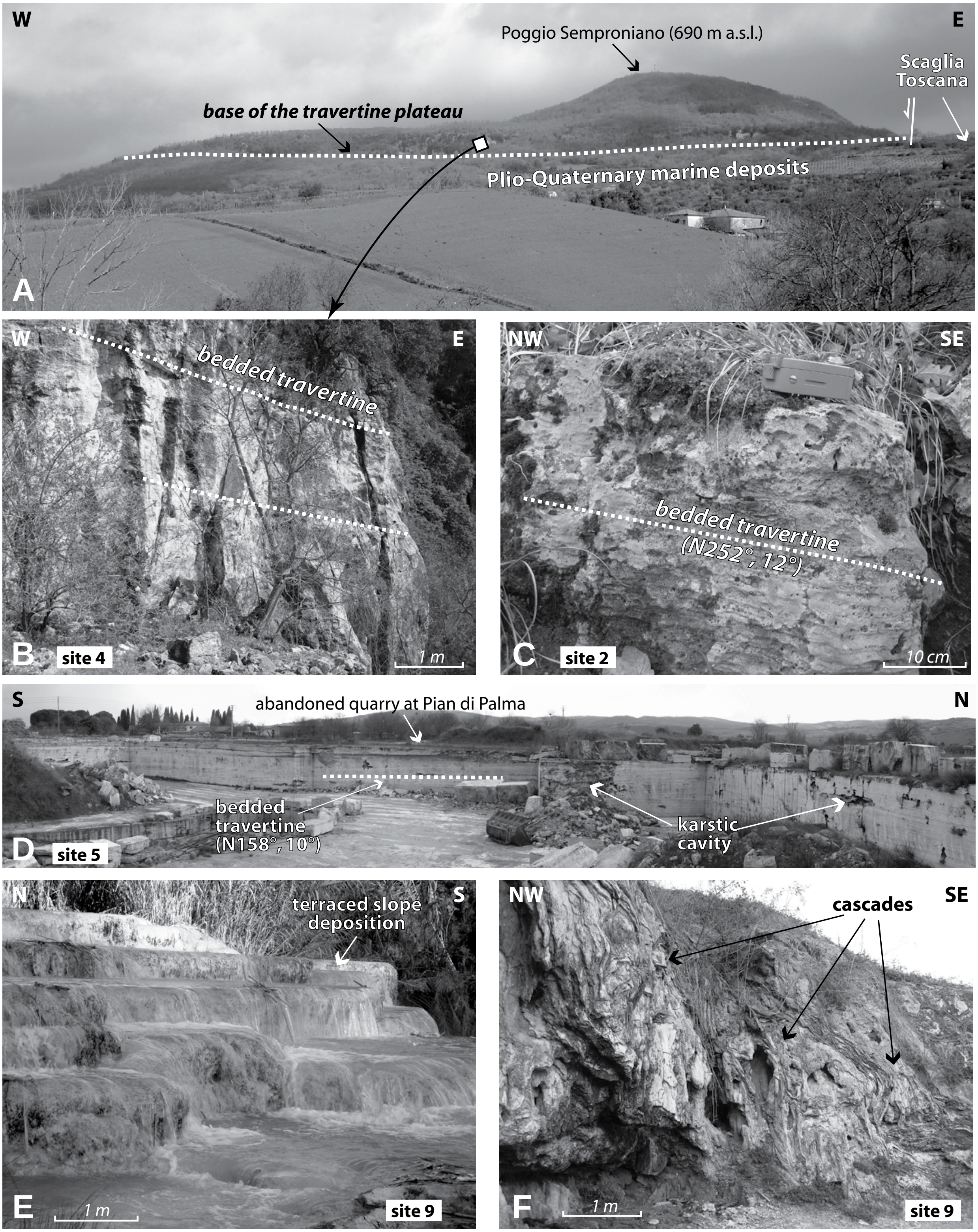

Figure 6. (A) Panoramic view of the Poggio Semproniano travertine plateau lying on top of the Pliocene–Quaternary marine deposits and bounded, toward the east, by a major N-S–striking extensional fault. In the fault footwall, the Scaglia Toscana Formation (belonging to the Tuscan Nappe) is exposed. (B) Subhorizontal, meter-thick bedding of the travertine deposit forming the plateau of Poggio Semproniano. (C) Close-up view of the bedded travertine occurring at Poggio i Piani. (D) Bedded travertine exposed within the abandoned quarry of the Pian di Palma locality. The travertine deposit is characterized by subhorizontal beds affected by karst cavities. (E) Travertine terraces with active deposition from $CaCO_3$-rich thermal waters near the public thermal center in Bagni di Saturnia. (F) Recent fossil travertine waterfalls near Saturnia. Color version is available as part of the data repository item (see text footnote 1).

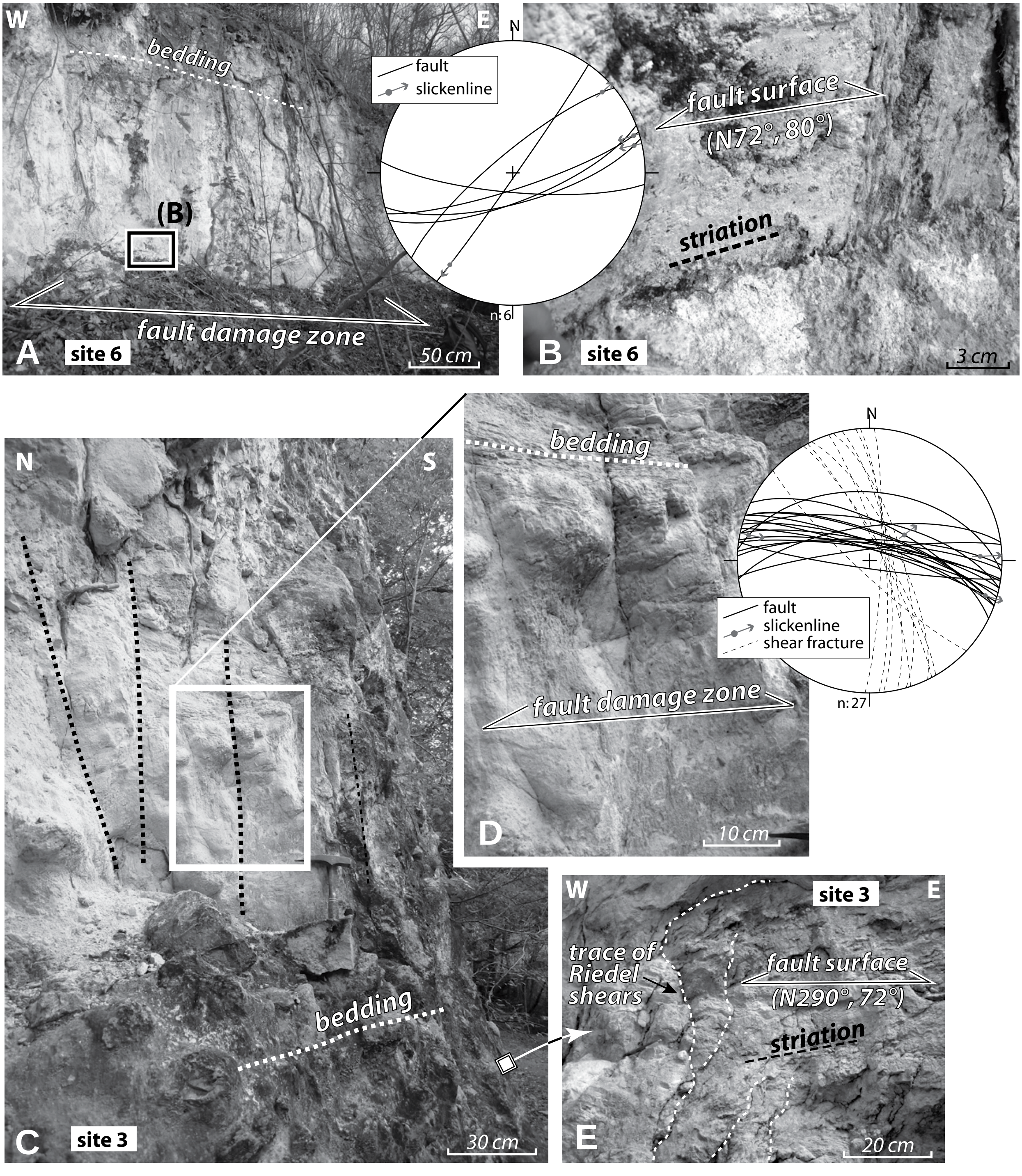

Figure 7. E-W–striking, right-lateral, strike-slip faults affecting the bedded travertine at (A–B) Poggio Pancotta and (C–E) Poggio Semproniano. (A) At Poggio Pancotta, a meter-wide fault damage zone and narrowly spaced (in the order of a few decimeters) fault surfaces occur within the travertine deposit. (B) Fault surfaces are equipped with oblique- to strike-slip striations (pitch is generally higher than 160° or lesser than 20°; see the stereoplot). (C) The fault damage zone across travertine beds at Poggio Semproniano is characterized by highly dipping surfaces (see the stereoplot). (D) Meter-wide fault cataclastic bands consisting of severely fractured travertine blocks and decimeter-spaced fault surfaces. (E) Fault systems include curvilinear shear surfaces making an angle of 20°–25° with the strike of the main fault surface and interpreted as Riedel shears within a right-lateral strike-slip kinematic structure. Arrows of slickenlines in stereoplots indicate hanging-wall movement. Color version is available as part of the data repository item (see text footnote 1).

affecting the Pleistocene continental deposits exposed to the southeast of Semproniano (site 12). These faults consist of fault segments (Fig. DR1B) with spacing of a few decimeters and displacement of a few centimeters at the most. When present, fault striations show a pitch around 160° (Fig. DR1B), indicating oblique strike-slip kinematics. Subsidiary Riedel shears are consistent with right-lateral fault motions. Furthermore, this fault set is aligned along the strike of a main strike-slip fault zone exposed in an abandoned quarry within the Diaspri Formation (site 11; Fig. DR1C). This NW-SE–striking fault zone is characterized by near-vertical fault surfaces, forming a negative flower structure, close to which bedding is severely undulated and verticalized.

Calcite-Filled Veins

At Poggio Semproniano (site 13), calcite-filled veins occur as a systematic set cutting through the bedded travertine and the underlying Scaglia Toscana Formation. These veins are 2–5 cm thick, with variable spacing between ~0.1 m and 1 m (Fig. 9A). The veins consist of monogenic filling of white crystalline calcite or rhythmic millimeter-thick white-and-gray layering (Figs. 9B and 9C). At Poggio Semproniano, this vein set strikes NW-SE (average strike: N129°) and dips steeply (>70°) toward the SW (Fig. 9A).

Fractures

At Semproniano (site 1), Poggio i Piani (site 2), Poggio Semproniano (site 4), and Pian di Palma (site 10), travertine deposits are affected by networks of fractures, some of which are strongly karstified. Fractures consist of decimeter-wide mechanical discontinuities within the travertine beds with either curvilinear or planar geometries. Fractures are commonly identified around (several meters from) the main fault systems cutting through the travertine bodies. At Poggio Semproniano and Poggio i Piani, these features strike from ESE-WNW to ENE-WSW, with dip angles close to 90° (Fig. DR1D). Evidence of karst weathering is common along the fracture surfaces, which consist of central cracks surrounded by several secondary anastomosing irregular fractures. The edges of these fractures are often karstified with a typical jigsaw profile. In the I Pianetti quarry, the karst fractures strike NE-SW. These features are meters to decameters long, with a mean spacing of 5–10 m (Fig. 9D). Karstified fractures are often connected, upward or downward, with large subhorizontal cavities. Locally, these fractures host speleothems formed by sparry and globular calcite (Fig. 9E).

Banded Travertine through Travertine Beds

At Saturnia (site 8), an exposed steeply dipping, 0.5-m-thick banded travertine cuts through the subhorizontal travertine beds (Fig. 10A). The banded travertine forms an inclined (~33°) tabular body striking N282° and consists of fine-grained white carbonate concretions forming centimeter-thick bands parallel to the contact with the host travertine beds (Fig. 10B). Similar geometrical and crosscutting relationships have been observed within the travertine exposed to the north of the village of Saturnia (site 7), where a meter-thick banded travertine characterized by undulating bands cuts through the bedded travertine (Fig. DR1E).

$^{230}Th/^{234}U$ Geochronology

Eighteen banded and bedded travertine samples, calcite-filled veins, and speleothem-like concretions were analyzed to constrain the age of

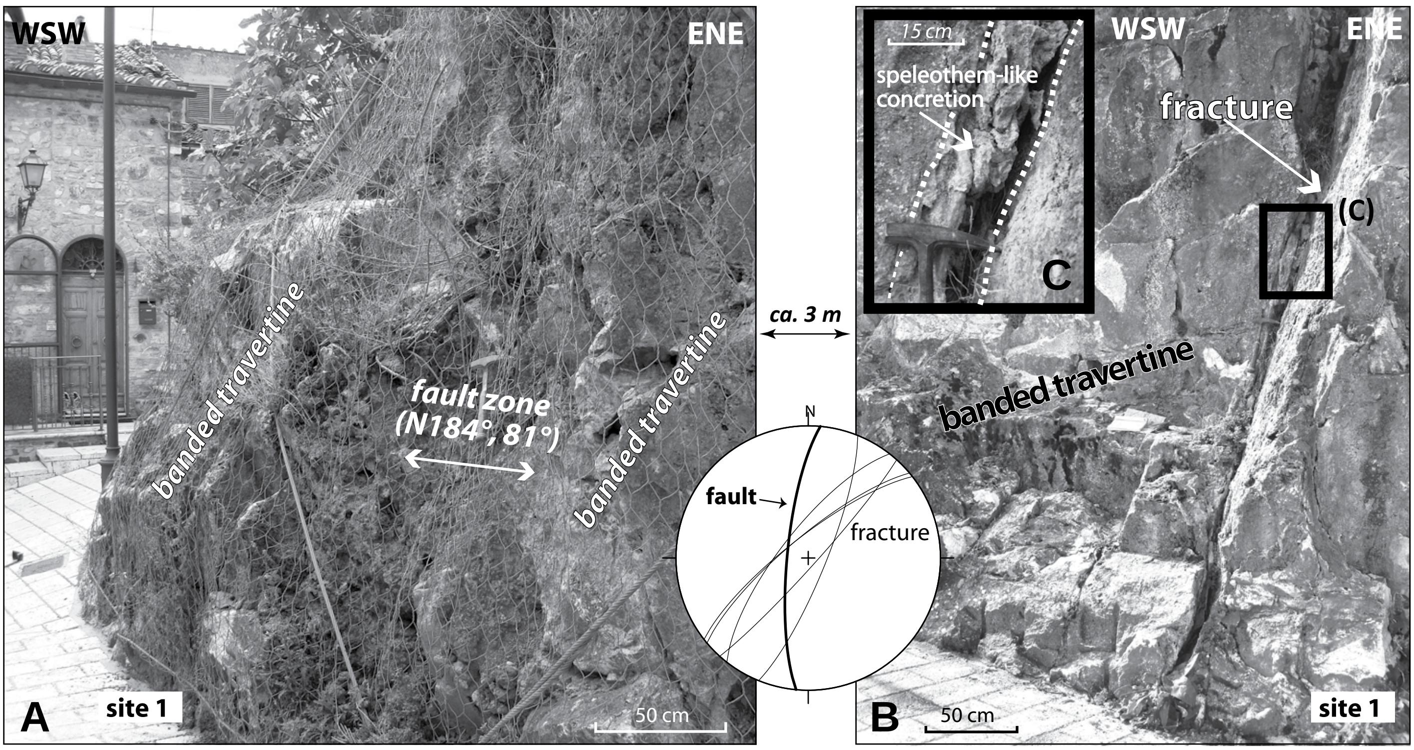

Figure 8. (A) N-S–striking fault across the banded travertine of the Semproniano village. The fault is characterized by a half-meter-wide damage zone. (B) NE-SW–striking fractures, correlated to the N-S–striking fault, cut through the banded travertine. (C) Fractures are filled by speleothem-like concretions. Geometrical relationships between fault surface and speleothem-filled fractures suggest an oblique shear for this extensional fault (see the stereoplot, stereographic projection, Schmidt net, lower hemisphere). Color version is available as part of the data repository item (see text footnote 1).

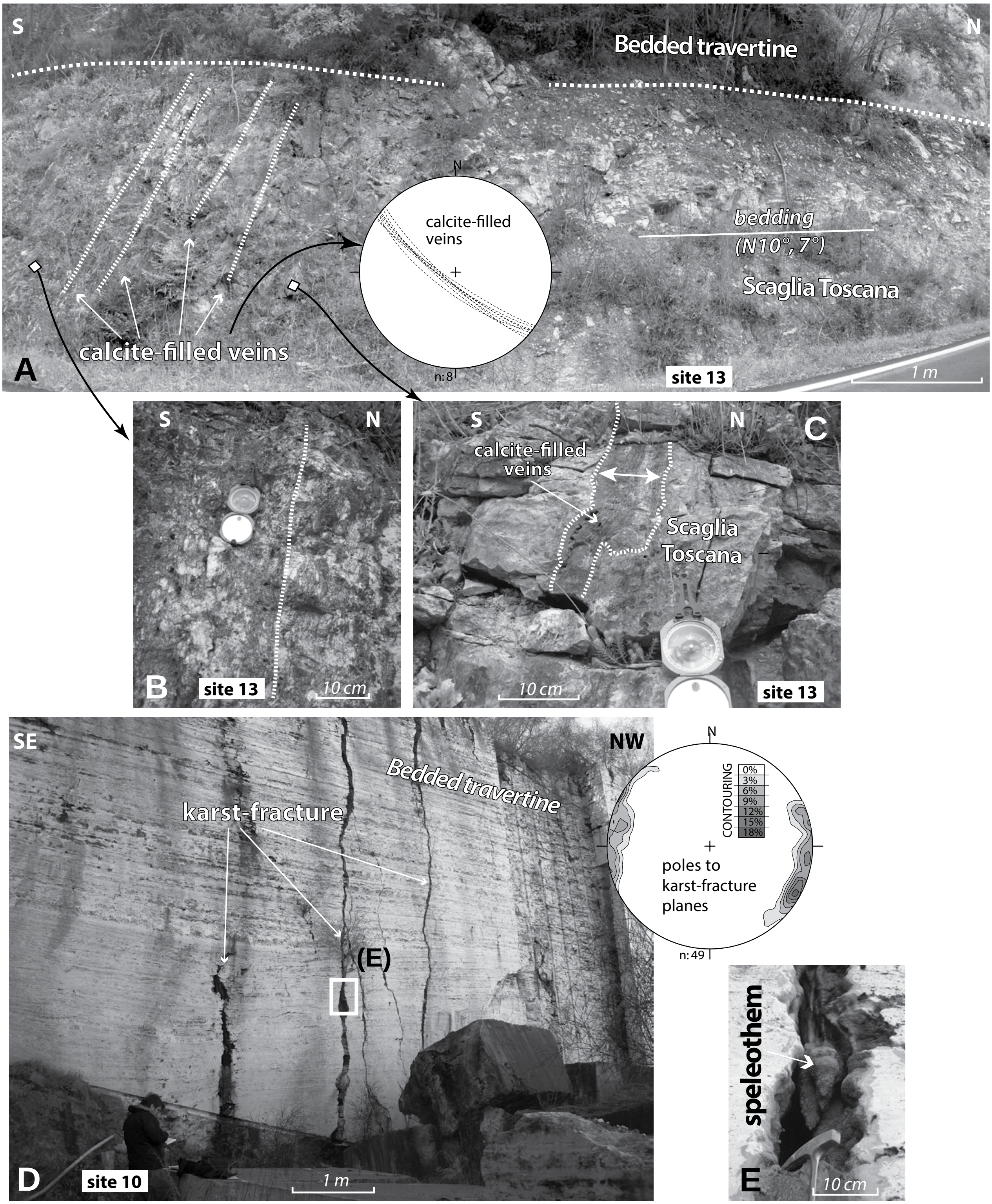

Figure 9. (A) Set of calcite-filled steep veins cutting through the subhorizontal Scaglia Toscana Formation lying below the bedded travertine of Poggio Semproniano. The veins strike NW-SE and dip toward the SW (see the stereoplot, stereographic projection, Schmidt net, lower hemisphere). These features consist of both (B) centimeter-thick monogenic calcite-filled veins and (C) decimeter-thick rhythmic layering of white-and-gray levels. (D) NNE-SSW–striking (see the stereoplot, stereographic projection, Schmidt net, lower hemisphere) karstified fractures across bedded travertine exposed in the I Pianetti quarry. (E) Close-up view of D showing a speleothem occurring within a karstified fracture. Color version is available as part of the data repository item (see text footnote 1).

hydrothermal circulation in the Albegna basin. The samples were analyzed at the Laboratory of Environmental and Isotopic Geochemistry (Department of Sciences, Roma Tre University, Italy). Samples were cut with a diamond saw and ultrasonically washed in deionized water. About 60 g of each prepared sample were dissolved in 7 *N* HNO_3 and filtered to separate leachates from insoluble residue. The leachates were heated to 200 °C after adding a few milliliters of hydrogen peroxide to annihilate organic matter, and then spiked with a $^{228}Th/^{232}U$ tracer. The isotopic complexes of U and Th were extracted according to the procedure described in Edwards et al. (1987) and then analyzed through alpha-counting using high-resolution ion-implanted Ortec silicon-surface barrier detectors. For samples with a $^{230}Th/^{232}Th$ activity ratio higher than 80 (free from nonradiogenic ^{230}Th), ages were determined using the measured $^{230}Th/^{234}U$ and $^{234}U/^{238}U$ activity ratios. Sample ages characterized by a $^{230}Th/^{232}Th$ activity ratio less than or equal to 80, indicating the presence of nonradiogenic (detrital) ^{230}Th, required a correction based on the assumption of an average $^{230}Th/^{232}Th$ activity ratio of 0.85 ± 0.36 for all detrital Th (Wedepohl, 1995). All ages were finally calculated using Isoplot (Ludwig, 2003) with errors expressed as ±1σ.

Our $^{230}Th/^{234}U$ geochronological data are reported in Table 3. All samples show low U concentrations ranging from 3 to 208 ppb, with a $^{234}U/^{238}U$ activity ratio between 0.978 and 1.585. The $^{230}Th/^{232}Th$ activity ratios, which indicate the extent of detrital contamination in the analyzed samples, range between 1.2 and 289. Determined ages span within the 33–214 ka interval. The youngest ages were obtained for bedded travertine at Pian di Palma quarry (33 ± 4 and 49 ± 15 ka) and Bagni di Saturnia (40 ± 7 ka), and for a calcite vein at Poggio Semproniano (39 ± 4 ka). The oldest ages were obtained for the bedded travertine at Semproniano village (214 +50/–37 ka), Poggio I Piani (198 ± 18 ka), and Poggio Semproniano (171 ± 19 ka). Moreover, three ages were older than the limit (ca. 350 ka) of the dating method. These ages are those of the banded travertine at the Semproniano village and I Vignacci localities (Table 3).

Carbon and Oxygen Isotopes and Calculated Paleofluid Temperatures

Carbon- and oxygen-isotope ($\delta^{13}C$ and $\delta^{18}O$) analyses on 38 samples were performed to constrain the chemistry of the parental hydrothermal fluid. Isotopic compositions were measured according to the carbonate-specific method described in detail in Breitenbach and Bernasconi (2011). Approximately 100 µg of powder were placed into 12 mL Exetainers, (Labco, High Wycombe, UK) and flushed with pure helium. The samples were reacted with 3–5 drops of 100% phosphoric acid at 70 °C with a Thermo Fisher GasBench device connected to a Thermo Fisher Delta V mass spectrometer. The average long-term reproducibility of the measurements (based on replicated standards) is ±0.05‰ for $\delta^{13}C$ and ±0.06‰ for $\delta^{18}O$. The instrument was calibrated with the international standards NBS19 ($\delta^{13}C$ = 1.95‰ and $\delta^{18}O$ = –2.2‰) and NBS18 ($\delta^{13}C$ = –5.01‰ and $\delta^{18}O$ = –23.01‰). Results are expressed in the conventional delta notation (in ‰) against the Vienna Peedee belemnite (VPDB) standard for both $\delta^{13}C$ and $\delta^{18}O$. Formation temperatures of the travertines were determined with the equation of Kele et al. (2015), which is based on travertine vent and pool samples. Calculations were run using the present-day $\delta^{18}O$ value of the Bagni di Saturnia hydrothermal spring (–6.4‰ Vienna standard mean ocean water [VSMOW]), which is characterized by a constant temperature of 37 °C (e.g., Minissale, 2004). The oxygen-isotope composition of the travertine precipitating water is therefore assumed to have been similar to that of the presently active spring at Bagni di Saturnia. Stable-isotope composition and calculated paleotemperatures are reported in Table 4 and Figure 11.

Selected samples include banded travertines, bedded travertines, calcite-filled veins, and speleothem-like concretions. With the exception of light-brown speleothem-like concretions in secondary fractures occurring at Semproniano (SPV1 and SPV2; Fig. 8C), all travertines and associated mineralizations showed positive $\delta^{13}C$ values between 2.8‰ and 10.5‰ (mean value 6.7‰), indicating a thermogene origin (Pentecost, 2005). The $\delta^{18}O$ values are between −12.7‰ and −5.1‰ (VPDB), with a mean value −8.64‰ (Figs. 11A and 11B).

Calculated paleotemperatures range between a minimum of 22 °C and a maximum of 60 °C (Table 4). Samples characterized by the highest calculated paleotemperatures belong to Semproniano village fissure ridge banded travertines, whereas the lowest ones belong to bedded travertines from Pian di Palma quarry. This evidence attests to a trend of decreasing paleotemperature moving from highest to lowest elevations and from north to south in the study area (Figs. 11C and 11D). Banded travertines are

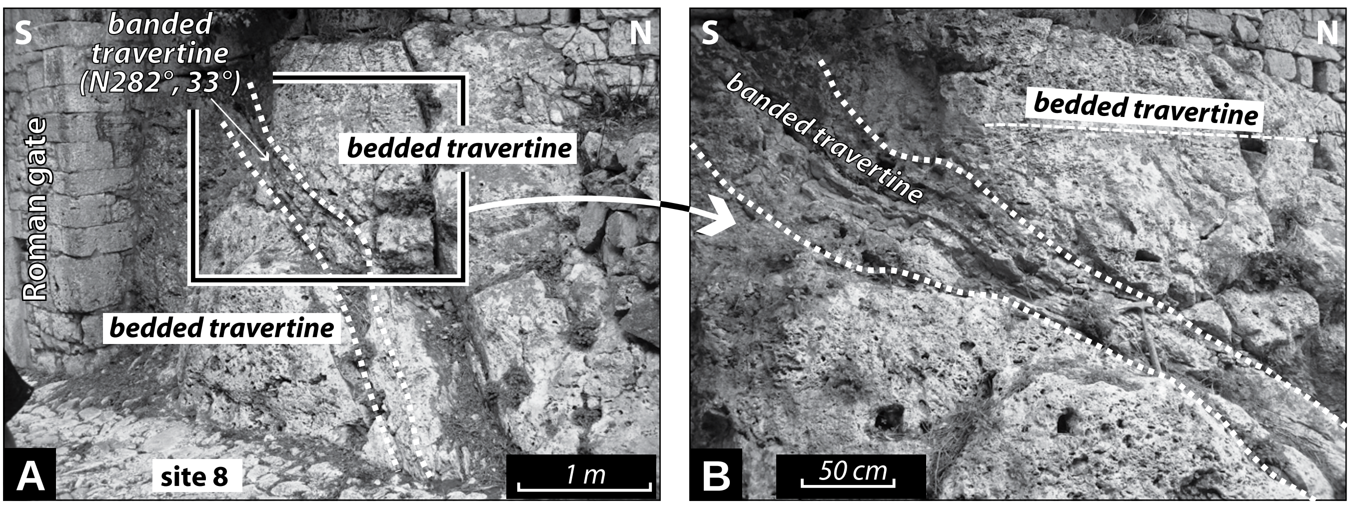

Figure 10. (A) Banded-bedded travertine relationships observed in the Saturnia travertine plateau near the Roman gate (Saturnia village, site 8). (B) Decimeter-thick banded travertine crosscuts the subhorizontal bedded travertine (Saturnia village, site 8). Color version is available as part of the data repository item (see text footnote 1).

TABLE 3. FABRIC TYPE, URANIUM ABUNDANCE, URANIUM AND THORIUM ACTIVITY RATIOS, AND AGES OF SAMPLES (TRAVERTINE AND CALCITE-FILLED VEINS) FROM THE ALBEGNA BASIN

Location	Sample	Rock type	U (ppm)	$^{230}Th/^{232}Th$	$^{234}U/^{238}U$	$^{230}Th/^{234}U$	($^{230}Th/^{234}U$) corrected*	Age (ka)
Semproniano village	SP1	Banded travertine	0.0124 ± 0.0009	23.746 ± 2.639	1.138 ± 0.107	1.014 ± 0.087		>350
Semproniano village	SP8	Banded travertine	0.0152 ± 0.0004	14.516 ± 1.511	0.980 ± 0.034	1.016 ± 0.043		>350
Semproniano village	SPV1	Speleothem-like	0.145 ± 0.004	125.34 ± 45.73	1.003 ± 0.028	0.588 ± 0.034		97 ± 9
Semproniano village	SP11	Bedded travertine	0.0 53 ± 0.002	7.148 ± 0.251	1.094 ± 0.026	0.892 ± 0.027	0.878 ± 0.051	214 +50/–37
Vignacci	VI1	Banded travertine	0.0770 ± 0.0006	2.277 ± 0.112	1.012 ± 0.071	1.578 ± 0.093		>350
Poggio Semproniano	SP10	Calcite vein	0.032 ± 0.002	110.353 ± 20.338	0.978 ± 0.061	0.299 ± 0.023		39 ± 4
Poggio Semproniano	PO2	Bedded travertine	0.053 ± 0.002	169.884 ± 26.205	1.198 ± 0.036	0.818 ± 0.039		171 ± 19
Poggio i Piani	PP1	Bedded travertine	0.077 ± 0.003	171.43 ± 23.82	1.112 ± 0.031	0.857 ± 0.028		198 ± 18
Pian di Palma Quarry	USI13 1-7	Bedded travertine	0.031 ± 0.002	107.279 ± 80.071	1.403 ± 0.125	0.263 ± 0.026		33 ± 4
Pian di Palma Quarry	USI1	Bedded travertine	0.0121 ± 0.0007	21.875 ± 5.503	1.449 ± 0.104	0.378 ± 0.034	0.369 ± 0.093	49 ± 15
Saturnia village	SA1	Bedded travertine	0.129 ± 0.014	289 ± 175	1.125 ± 0.053	0.736 ± 0.045		140 ± 17
Saturnia village	SA14-05	Bedded travertine	0.208 ± 0.005	26.373 ± 1.568	1.133 ± 0.020	0.749 ± 0.023	0.742 ± 0.060	142 ± 23
Saturnia village	SA14-01	Banded travertine	0.018 ± 0.001	21.830 ± 3.061	1.565 ± 0.056	0.613 ± 0.024	0.603 ± 0.078	94 ± 18
Saturnia village	SA2	Banded travertine	0.0130 ± 0.0009	87.275 ± 12.583	1.585 ± 0.098	0.696 ± 0.053		118 ± 15
Bagni di Saturnia	SA6	Bedded travertine	0.01000 ± 0.0006	1.234 ± 0.106	1.531 ± 0.116	0.490 ± 0.039	0.312 ± 0.047	40 ± 7
I Pianetti Quarry	ST4	Bedded travertine	0.022 ± 0.002	1.226 ± 0.081	1.361 ± 0.073	0.785 ± 0.041	0.648 ± 0.056	107 ± 15
I Pianetti Quarry	ST1	Bedded travertine	0.045 ± 0.003	5.823 ± 0.482	1.196 ± 0.035	0.746 ± 0.037	0.716 ± 0.072	130 ± 23
I Pianetti Quarry	CP13-1-4	Bedded travertine	0.0095 ± 0.0005	3.186 ± 0.209	1.307 ± 0.063	0.681 ± 0.029	0.629 ± 0.049	103 ± 13

*The $^{230}Th/^{234}U$ ratio was corrected using the crustal thorium mean composition, 0.85 ± 0.36 (Wedepohl, 1995), for samples with a $^{230}Th/^{232}Th$ activity ratio lower than 80.

TABLE 4. STABLE OXYGEN- AND CARBON-ISOTOPE COMPOSITIONS, AND PALEOTEMPERATURES OF BANDED TRAVERTINE, BEDDED TRAVERTINE, AND CALCITE VEINS FROM THE ALBEGNA BASIN

Sample	Location	Rock type	$\delta^{13}C$ (‰, VPDB)	$\delta^{18}O$ (‰, VPDB)	$\delta^{18}O$ (‰, VSMOW)	$T_{calculated}$ (°C)
SP1	Semproniano village	Banded travertine	9.5	–12.7	17.8	60 ± 6
SP5	Semproniano village	Banded travertine	8.9	–10.8	19.8	49 ± 4
SP6	Semproniano village	Banded travertine	10.0	–12.2	18.3	57 ± 5
SP7	Semproniano village	Banded travertine	10.5	–11.6	19.0	53 ± 5
SP8	Semproniano village	Banded travertine	9.7	–12.3	18.2	57 ± 5
SP11	Semproniano village	Bedded travertine	9.9	–8.2	22.2	36 ± 2
SP14/06	Semproniano village	Bedded travertine	5.3	–9.8	20.9	44 ± 3
SP14/05	Semproniano village	Bedded travertine	5.8	–9.7	20.9	44 ± 3
SPV1	Semproniano village	Speleothem-like	–9.4	–6.0	25.6	n.c.
SPV2	Semproniano village	Speleothem-like	–9.7	–5.6	23.7	n.c.
PP1	Poggio i Piani	Bedded travertine	6.5	–11.6	19.0	53 ± 5
PS 1	Poggio Semproniano	Bedded travertine	6.9	–10.2	20.4	46 ± 4
PS 3	Poggio Semproniano	Bedded travertine	5.8	–10.1	20.5	46 ± 4
SP9	Poggio Semproniano	Bedded travertine	6.8	–9.6	21.0	43 ± 3
PO1	Poggio Semproniano	Bedded travertine	5.6	–11.4	19.2	53 ± 5
PO2	Poggio Semproniano	Bedded travertine	7.1	–9.8	20.8	44 ± 3
SP10	Poggio Semproniano	Calcite vein	8.4	–10.7	19.9	49 ± 4
SP3	Poggio Semproniano	Calcite vein	7.1	–11.5	19.0	53 ± 5
SA1	Saturnia village	Bedded travertine	7.3	–7.5	23.2	33 ± 2
SA14/05	Saturnia village	Bedded travertine	6.4	–8.0	22.6	36 ± 2
SA14/01	Saturnia village	Banded travertine	7.5	–9.1	21.6	41 ± 3
SA2	Saturnia village	Banded travertine	7.7	–9.1	21.6	41 ± 3
SA5	Saturnia Spring	Bedded travertine	2.8	–8.7	22.0	38 ± 2
SA6	Saturnia Spring	Bedded travertine	3.1	–6.6	24.1	29 ± 2
SA7	Saturnia Spring	Bedded travertine	3.3	–8.1	22.6	36 ± 2
USI13-1-1	Pian di Palma quarry	Bedded travertine	7.4	–5.2	25.6	22 ± 1
USI13-1-2	Pian di Palma quarry	Bedded travertine	7.4	–5.2	25.6	22 ± 1
USI13-1-3	Pian di Palma quarry	Bedded travertine	5.8	–5.8	24.9	25 ± 1
USI13-1-4	Pian di Palma quarry	Bedded travertine	6.2	–5.4	25.3	24 ± 1
USI13-1-5	Pian di Palma quarry	Bedded travertine	6.2	–5.4	25.4	23 ± 1
USI13-1-6	Pian di Palma quarry	Bedded travertine	7.1	–5.1	25.6	22 ± 1
CP 13-1-1	I Pianetti quarry	Bedded travertine	6.5	–6.1	24.6	26 ± 1
CP 13-1-2	I Pianetti quarry	Bedded travertine	6.2	–6.3	24.4	27 ± 1
CP 13-1-3	I Pianetti quarry	Bedded travertine	6.4	–6.2	24.6	27 ± 1
CP 13-1-4	I Pianetti quarry	Bedded travertine	6.2	–6.8	23.9	30 ± 2
CP18-01	I Pianetti quarry	Bedded travertine	6.5	–7.9	22.8	35 ± 2
CP18-02	I Pianetti quarry	Bedded travertine	5.1	–8.0	22.7	35 ± 2
CP18-03	I Pianetti quarry	Bedded travertine	6.1	–7.9	22.8	35 ± 2

Note: Isotope compositions are expressed in ‰ relative to Vienna Peedee belemnite standard (VPDB). Temperature of parental fluids was derived from $\delta^{18}O$ through the equation of Kele et al. (2015). VPDB—Vienna Peedee belemnite standard; VSMOW—Vienna standard mean ocean water; n.c.—not calculated.

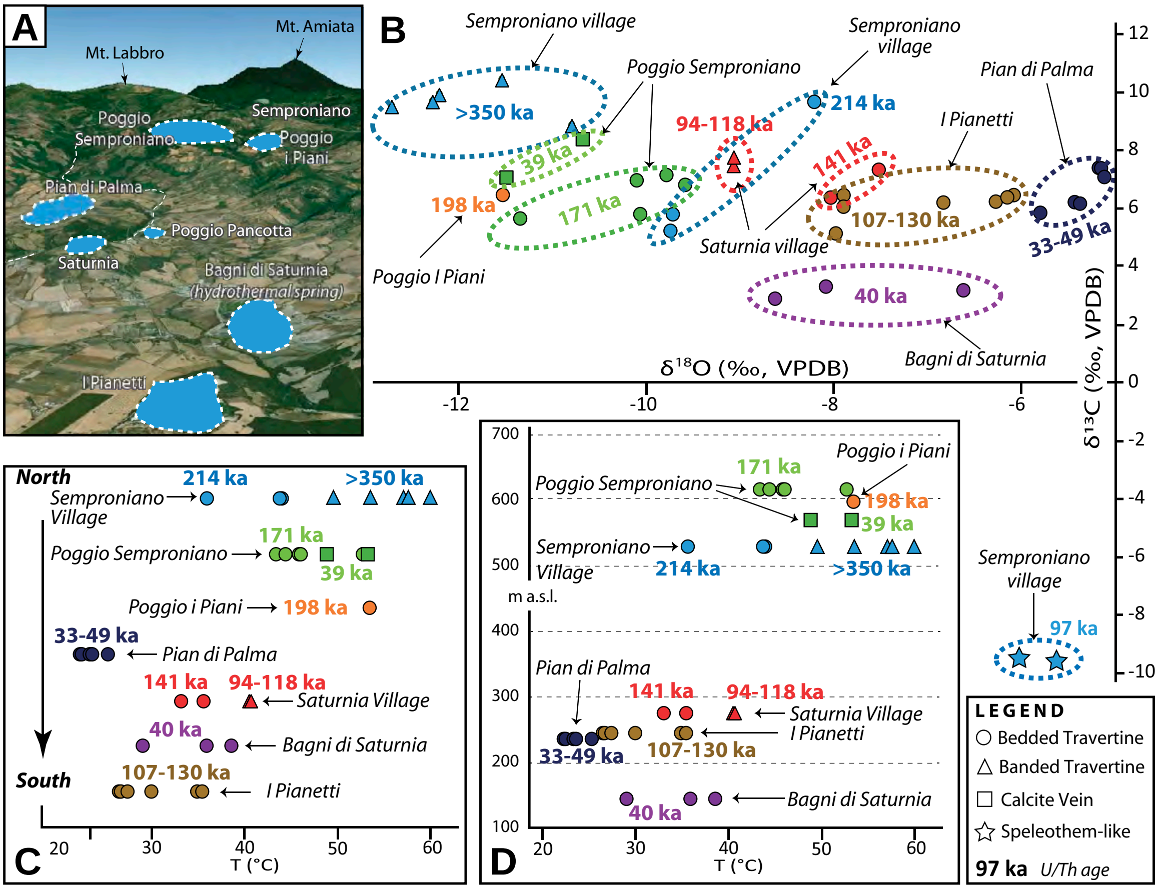

Figure 11. (A) Northward panoramic view (Google Earth image similar to Fig. 4A) with locations of the studied travertine deposits. (B) Combined plot of $\delta^{13}C$ (‰, VPDB) and $\delta^{18}O$ (‰, VPDB) isotope values obtained for the samples of bedded and banded travertines, calcite veins, and speleothem-like concretions. Isotope values are correlated with the corresponding U/Th ages. (C) Parental fluid temperatures of the studied travertine deposits plotted versus the geographic location of the corresponding travertine deposits and correlated with the corresponding U/Th ages (Tables 3 and 4). (D) Parental fluid temperatures of the studied travertine deposits plotted versus the elevations of the corresponding travertine deposits and correlated with the corresponding U/Th ages.

generally characterized by mean calculated paleotemperatures of around 10 °C higher than the associated bedded travertine.

DISCUSSION

Tectonic Synthesis

The main travertine deposits within the Albegna basin are aligned N-S (Fig. 3A) and are located along major N-S–striking faults or at fault intersections (at Semproniano village, Poggio Semproniano, Poggio I Piani). Our structural analysis documents that the travertine deposits of Poggio Semproniano and Poggio Pancotta are crosscut by right-lateral strike-slip faults oriented E-W and WNW-ESE, respectively. In addition, we documented a N-S–striking fault at Semproniano village that cuts through the fissure ridge with an oblique-extensional shear. This fault pattern of N-S– and E-W–striking faults is similar to nearby hydrothermal areas in southern Tuscany (e.g., Brogi et al., 2010a, 2012; Rimondi et al., 2015) and along the Tyrrhenian margin (see following).

Our geochronological data allow dating of the tectonic-hydrothermal process. The oldest travertines and veins are older than the limit of the dating method (ca. 350 ka), whereas the youngest inactive deposit, at the Pian di Palma quarry, is ca. 33 ka in age. The Albegna basin hydrothermal system and associated travertine deposition are still active at Bagni di Saturnia. Integrating previous data from nearby similar hydrothermal settings (Taddeucci and Voltaggio, 1987; Brogi et al., 2012; Rimondi et al., 2015), we can link the middle Pleistocene onset of hydrothermal activity in southern Tuscany with the main phases of crustal uplift and emplacement of magmatic bodies in the region (Barberi et al., 1994), with the volcanic activity of the Mount Amiata (300–190 ka; Cadoux and Pinti, 2009) and Vulsini Mountains (590–127 ka; Nappi et al., 1995), and with hypogenic speleogenesis (69–19 ka; Piccini et al., 2015). This hydrothermal scenario is consistent with the occurrence of a regional thermal anomaly below the Tuscan magmatic province, producing long-lived convective circulation of endogenic fluids during the Pleistocene (Minissale, 2004).

The relationships between travertine deposition and development of fault-fracture systems can be used to constrain the minimum age of faulting in the region. The E-W–striking right-lateral fault at Poggio Semproniano cut through the bedded travertine dated at 171 ± 19 ka, whereas the N-S–striking fault cut through the banded travertine at Semproniano fissure ridge dated as >350 ka. Tension fractures at the Semproniano fissure ridge are filled by speleothem-like concretions dated 97 ± 9 ka. The karstified fractures at Poggio I Piani and I Pianetti cut through bedded travertine dated 198 ± 18 ka and 107 ± 15 ka, respectively. These ages constrain the tectonic activity in the Albegna basin to the late Pleistocene.

In synthesis, our structural data show that, while travertine deposition within the study region is still active, fossil travertine deposits as young as 170 ka are crosscut by faults. All together, this evidence indicates that travertine deposition can be considered as syntectonic at the regional (basin) scale. If integrated with ages from recent studies (e.g., Brogi, 2008; Brogi et al., 2010a, 2014), our U-Th data show that faulting in southern Tuscany is significantly younger than previously thought and has worked simultaneously with long-lived convective circulation of hydrothermal fluids in the Tuscan magmatic province.

Hydrothermalism

In our data set (Table 4; Fig. 11), only the speleothem-like concretions sampled in some fractures (SPV1 and SPV2) are characterized by negative $\delta^{13}C$ values of −9.4‰ and −9.7‰, respectively. These negative values are probably due to the high contribution of atmospheric and soil-derived CO_2, suggesting carbonate mineralizations by percolation of meteoric waters within cracks (Pentecost, 2005). This suggests that the SempronIano fissure ridge was probably fully formed at 97 ka, which is the time of deposition of the analyzed speleothem-like concretions. On the other hand, the travertine and veins have positive $\delta^{13}C$ values (Table 4), indicative of mixing of deep magmatic fluids with meteoric waters having CO_2 originating from limestone decarbonation (Gonfiantini et al., 1968; Guo et al., 1996). Our $\delta^{13}C$ and $\delta^{18}O$ values are comparable with those reported in previous studies (e.g., Minissale, 2004, and references therein) and are in the range typical of thermogene travertines deposited by present-day thermal springs of central Italy (Minissale, 2004; Gandin and Capezzuoli, 2008). Travertines belonging to Semproniano village fissure ridge show $\delta^{13}C$ values more positive than usual thermogene values, likely attributable to downstream CO_2 degassing, producing an increase in $\delta^{13}C$ (Özkul et al., 2013).

Travertine deposits of the Albegna basin are hydrothermally distinct from nearby hydrothermal deposits along the Tyrrhenian margin. Continental carbonates of the Sarteano system (southern Tuscany) yielded $\delta^{13}C$ values ranging between −2.5‰ and 1.6‰ (Brogi et al., 2012), indicative of a larger meteoric component. The Tivoli travertine (Latium) shows a range of $\delta^{13}C$ between 8.31‰ and 10.77‰ and a range of $\delta^{18}O$ between −4.76‰ and −7.18‰, which were attributed to a strong process of diagenesis that obliterated the original oxygen-isotopic signature (Manfra et al., 1974; De Filippis et al., 2013a). The variability of oxygen- and carbon-isotope compositions observed in the travertines of the Albegna basin has analogies with those of travertine samples from the Denizli basin (Turkey) and Mammoth Hot Spring (Yellowstone Park, USA). For the Denizli basin, the travertine formation is largely attributed to variable interaction between the meteoric waters and the deep hydrothermal fluids (e.g., Dilsiz, 2006; Uysal et al., 2007; De Filippis et al., 2013a). In contrast, the travertine deposition at Mammoth Hot Spring is attributed to a high extent of CO_2 degassing during diagenetic processes (e.g., Fouke et al., 2000; Chafetz and Guidry, 2003). Based on carbon- and oxygen-isotope data, travertines of the Albegna basin can be interpreted as forming during dominant circulation of CO_2-enriched hydrothermal fluids with variable contributions of colder shallow aquifer fluids mainly recharged by meteoric precipitation.

Estimated fluid temperatures span from ~60 °C for the banded travertine from Semproniano to ~22 °C for the bedded travertine from the Pian di Palma quarry (Table 4; Figs. 11C and 11D). There are no analogous data for fossil hydrothermal deposits along the Tyrrhenian margin in central Italy, but our estimated temperatures are comparable with the temperatures of active thermal springs in this region (temperature > 20 °C; Minissale, 2004).

The longevity of individual travertine deposits and structures in the Albegna basin cannot be constrained with the available age data, but the activity of the entire Albegna hydrothermal-travertine system must be longer than 350 k.y. This is more than estimated activities at Rapolano (Tuscany, Italy, ~133 k.y.; Brogi et al., 2010a), at Sarteano (Tuscany, Italy, ~250 k.y.; Brogi et al., 2012), at Tivoli (Latium, central Italy, ~100 k.y.; Faccenna et al., 2008), at Limagne graben, France (Massif Central, ~250 k.y.; Rihs et al., 2000), and in the Ebro basin, Spain (~239 k.y.; Luque and Julià, 2007). Longer activities on the other hand, have been documented for travertine deposition in the Denizli basin, Turkey (at least 600 k.y.; Engin et al., 1999; Altunel and Karabacak, 2005; Uysal et al., 2007; De Filippis et al., 2013a Özkul et al., 2013; Lebatard et al., 2014; Toker et al., 2015), and in the Rio Grande rift, United States (~660 k.y.; Priewisch et al., 2014).

Spatio-Temporal Hydrothermal Evolution

We can interpret the travertine deposits of the Albegna basin as markers of hydrothermal activity that evolved in space and time along a N-S structural alignment. The following main features have been recognized and documented:

(1) There is a general southward rejuvenation of the hydrothermal system, i.e., the travertine deposition becomes younger moving from north to south. The Semproniano deposits have ages older than 350 ka, whereas the youngest dated deposit (ca. 40 ka) and the active springs occur toward the south in the Bagni di Saturnia locality.

(2) There is a decrease in travertine deposition from 600–700 m a.s.l. at Semproniano and Poggio Semproniano to 140–220 m a.s.l. at Bagni di Saturnia and I Pianetti. The parallel elevation and chronological gradients (from north to south) indicate a rapid lowering of the water table toward the south (i.e., toward the Tyrrhenian Sea) during Pleistocene time on the order of 1 mm yr^{-1} (Piccini et al., 2015).

(3) There is a change in isotopic signatures. Along the N-S profile (Fig. 11A), a general decreasing trend of $\delta^{13}C$ and increasing trend of $\delta^{18}O$ from older to younger travertine deposits (Fig. 11B) are observed. The only exceptions are the calcite-filled veins occurring at Poggio Semproniano, which developed synchronously with the bedded travertine of Bagni di Saturnia and Pian di Palma localities. The $\delta^{18}O$ values show a wide range, with the most negative values corresponding to older travertines (Semproniano village, Poggio Semproniano, and Poggio I Piani) and the less negative values belonging to the travertines of Pian di Palma quarry (the youngest deposit). The gradient of $\delta^{18}O$ values from north to south is interpreted as a decrease in temperature (Fig. 11C). This decreasing trend is also confirmed when considering the temperatures versus elevations of the travertine deposits (Fig. 11D). This evidence supports the hypothesis of an increasing contribution of meteoric waters with time.

Summarizing, we interpret the Albegna basin as a long-lived hydrothermal-tectonic setting with a progressive southward migration of the fluid circulation, moving away from the geothermal center of Mount Amiata, located to the north of the Albegna basin (Fig. 12). The main travertine-depositing center changed its position horizontally (along the N-S structural alignment) and vertically (lowering of the depositional elevations), reaching the present-day deposition center at the Bagni di Saturnia locality. The travertines show decreasing $\delta^{13}C$ and increasing $\delta^{18}O$ consistent with increasing dilution of endogenic fluids by meteoric fluids. The main extensional and strike-slip fault systems provided the necessary hydraulic pathways for infiltration of meteoric waters to the depth of the carbonate reservoir, the possible connection and mixing between different hydrogeological-hydrothermal circuits (e.g., Curewitz and Karson, 1997; Cox et al., 2001; Rowland and Sibson, 2004; Gudmundsson, 2011), and the subsequent ascension to surface of $CaCO_3$-rich hydrothermal fluids. Mixing

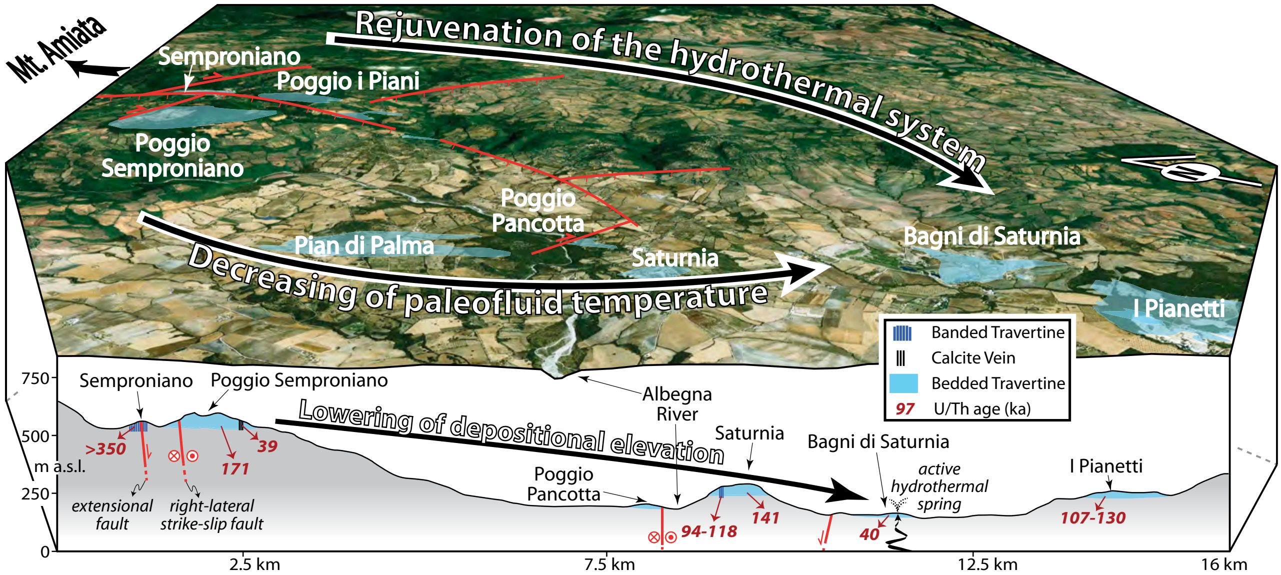

Figure 12. Spatio-temporal evolution of the hydrothermal system in the Albegna basin as constrained by the geological, geochronological, and geochemical datasets provided in this study (see also Piccini et al., 2015). The spatio-temporal evolution is characterized by younger travertines moving from north to south and from upper to lower elevations. The temperature of the travertine parental fluids decreases with time and space moving toward younger deposits, toward the south, and toward lower elevations of deposition. As explained in the text, $\delta^{13}C$ and $\delta^{18}O$ values also tend to change with space and time from north to south, from upper to lower elevations, and from older to younger deposits. Locations of the travertine deposits and travertine-related structures are also shown together with the fault pattern.

with meteoric fluids resulted in a decrease of fluid temperatures down to the present value of 37 °C at the Bagni di Saturnia springs (Minissale, 2004).

The Paleoclimate Influence

Our geochronological data can contribute to the understanding of the feedback relationships between thermogene travertine deposition and paleoclimate in the Albegna basin. In the last decades, many studies have been devoted to the correlation between travertine deposition and paleoclimate oscillations. There is a general consensus in considering warm and wet (interglacial) conditions as the most favorable for travertine deposition during late Quaternary time (e.g., Dramis et al., 1999; Frank et al., 2000; Rihs et al., 2000; Soligo et al., 2002; Pentecost, 2005; Luque and Julià, 2007; Faccenna et al., 2008; Kampman et al., 2012; Priewisch et al., 2014). Intuitively, highstand conditions of the water table during wet periods can favor the supply of fluids for the growth of travertine deposits (Rihs et al., 2000; Faccenna et al., 2008). Nevertheless, travertine formation in dry glacial periods (lowstand of the water table) has been documented and used to emphasize the importance of tectonic activity, rather than climate, to control travertine precipitation (e.g., Uysal et al., 2009; Brogi et al., 2010a; Özkul et al., 2013). Finally, complete interaction and feedbacks among fluid discharge, paleoclimate, and tectonics has been proposed by De Filippis et al. (2013a) to morphologically and volumetrically control the different travertine deposits (travertine plateaus and fissure ridges).

We compared the age of travertine deposition (Table 3) with major Quaternary paleoclimate indicators and events determined both at the global and regional scales (Fig. 13). We used, in particular, paleoclimate records extracted from the deep-sea oxygen-isotope trend (Zachos et al., 2001) integrated with the pollen data set from Valle di Castiglione (located ~200 km to the south of the Albegna basin; see location in Fig. 1). Although the travertine ages have rather large error bars, the majority of them fall within interglacial or interstadial periods. This suggests that the travertines and travertine-related structures preferentially formed during warm (and humid) climate periods characterized by highstand conditions of the water table. Nevertheless, our data also document that large volumetric amounts of travertine deposits in the Albegna basin (bedded travertine plateaus at Poggio Semproniano and at Saturnia village) were formed coeval with a glacial period at ca. 130–180 ka, which is also a nonhumid time, as demonstrated by the pollen curve from Valle di Castiglione (Fig. 13). This evidence probably indicates an important contribution of the endogenic fluid supply to travertine deposition during the lowstand (and nonhumid) conditions of the water table (see also Toker et al., 2015). In other words, the endogenic fluid supply may have partly compensated for the lowering of the water table during the glacial lowstand periods.

Insights on Tyrrhenian Margin Neotectonics

The recognized structural pattern of the Albegna basin is compatible with the postorogenic regional extensional tectonic regime described for the Tyrrhenian margin, where main NW-SE–striking extensional faults (i.e., parallel to the trend of the Apennines belt) and related sedimentary basins developed in Pliocene–Quaternary times (Malinverno and Ryan, 1986; Patacca et al., 1990; Bossio et al., 1993; Martini and Sagri, 1993; Bartole, 1995; Jolivet et al., 1998; Cavinato and De Celles, 1999; Pauselli et al., 2006; Billi and Tiberti, 2009; Brogi et al., 2014). Within this scenario, the strike-slip to transtensional faults oriented transversally to the NW-SE extensional boundary faults are interpreted as transfer systems accommodating different stretching rates within the extending crust (Faccenna et al., 1994; Aiello et al., 2000; Acocella and Funiciello, 2002, 2006; Liotta et al., 2015). It is worth nothing that many of these transverse faults have acted as preferential pathways for hydrothermal outflow and controlled distribution of volcanism along the Tyrrhenian margin at least since late Pleistocene time. In this regard, we report, from NW to SE along the Tyrrhenian margin, 10 main instances (see Fig. 14A) where

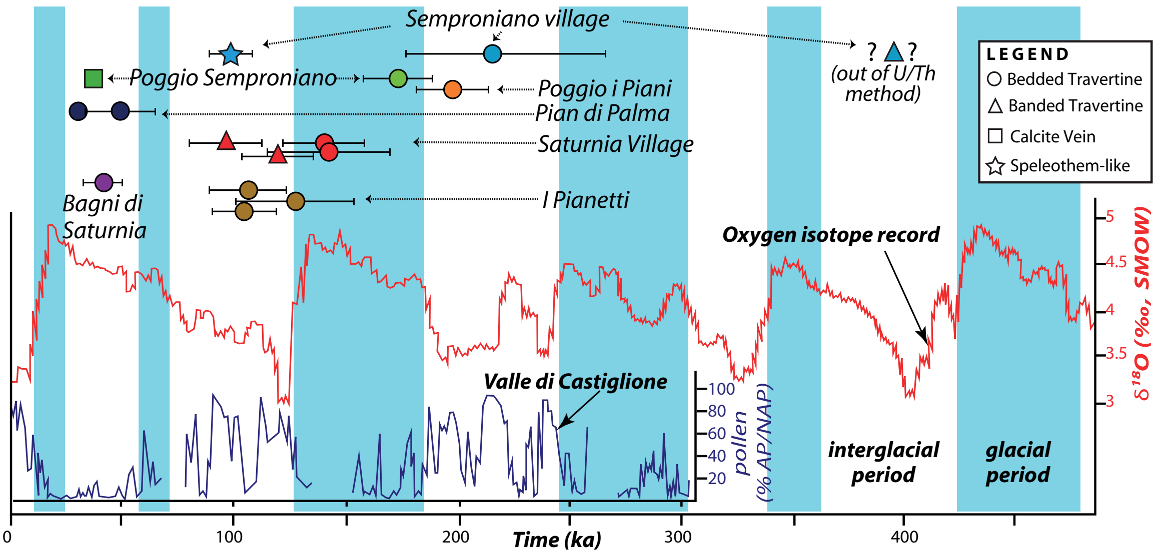

Figure 13. Comparison between U/Th ages of $CaCO_3$ samples (bedded and banded travertines, calcite-filled veins, and speleothem-like concretions) from the Albegna basin and major paleoclimate indicators represented by the deep-sea oxygen-isotope trend (Zachos et al., 2001) and the pollen data set from Valle di Castiglione (Tzedakis et al., 2001). Glacial-interglacial periods are redrawn and modified after Priewisch et al. (2014). Valle di Castiglione is located in central Italy (see location in Fig. 1) only ~200 km from the Albegna basin. AP—arboreal pollen; NAP—non-arboreal pollen.

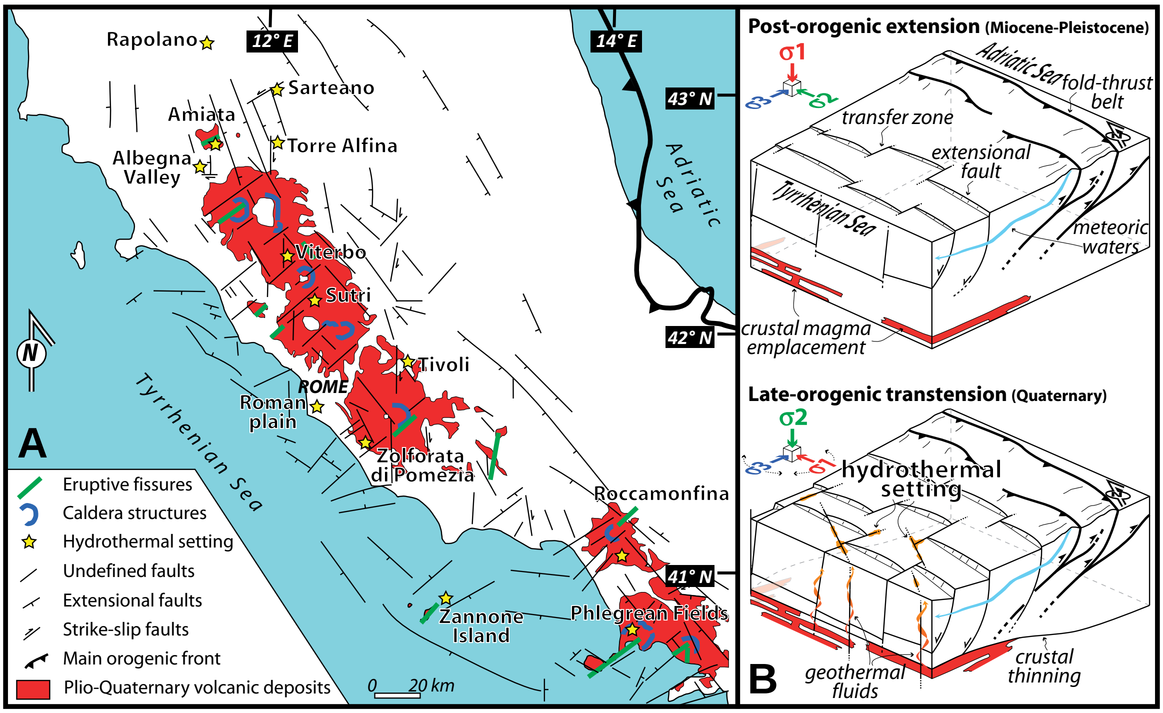

Figure 14. (A) Simplified structural map of the Tyrrhenian margin showing the main fault systems, the Pliocene–Quaternary volcanoes, and the principal hydrothermal-tectonic systems (redrawn and modified after Acocella and Funiciello, 2006; Conticelli et al., 2015). (B) Two-stage scenario (based on the model of Acocella and Funiciello, 2006) illustrating the structural control of the originally shallow transfer zones on the localization of hydrothermal fields. During postorogenic extension (above), the margin-transverse structures acted as non-Andersonian transfer zones restricted to shallow levels. Subsequently (below), due to the change in the stress tensor induced by crustal thinning (i.e., switch between σ_1 and σ_2 paleostress axes), these originally shallow faults were reactivated and enhanced so as to rupture downward into the crust and generate the pathway for hydrothermal fluid ascension.

recent or active hydrothermal activity is localized along transverse faults (i.e., NE-SW and N-S), as is the case of the Albegna basin (this study): (1) Rapolano, Tuscany (Brogi and Capezzuoli, 2009), (2) Sarteano, Tuscany (Brogi et al., 2012), (3) Torre Alfina, Latium (Vignaroli et al., 2013), (4) Roman Plain, Latium (Sella et al., 2014; Bigi et al., 2014; Frepoli et al., 2010), (5) Viterbo, Latium (Baldi et al., 1974; Chiocchini et al., 2010), (6) Sutri, Latium (Corrado et al., 2014), (7) Tivoli, Latium (Gasparini et al., 2002; Faccenna et al., 2008; De Filippis et al., 2013a, 2013b), (8) Zolforata di Pomezia, Latium (Vignaroli et al., 2015), (9) Zannone Island, Latium (Ingrassia et al., 2015), and (10) Mount Massico–Roccamonfina, Campania (Billi et al., 1997; Corniello et al., 2015).

Transfer faults are known as compartmental non-Andersonian faults restricted to shallow levels, i.e., in the hanging wall of extensional faults (Gibbs, 1984; van der Pluijm and Marshak, 2003). As such, transfer faults are not expected to act as pathways for endogenic (deep) hydrothermal fluids as is the case of the Albegna basin and elsewhere along the Tyrrhenian margin. We conclude that the structures that nucleated and initially grew as transfer zones oriented transversally to the Apennines trend (Neogene) have probably evolved as through-going crustal faults in recent times (Quaternary) so as to allow the upflow of endogenic fluids stored in geothermal reservoirs of the region. (1) In a first stage (Neogene; Fig. 14B), the postorogenic extensional tectonics that acted on the Tyrrhenian margin of the Apennines operated through major NW-SE–striking extensional faults. The orientation of the paleostress axes followed Anderson's theory of extensional faulting with a vertical σ_1 (maximum compression) direction and σ_2 and σ_3 (intermediate and minimum compression, respectively) directions lying on a horizontal plane. The vertical σ_1 direction was the consequence of far-field (slab retreat) and near-field (Apennines crustal thickening) stress regimes acting at the back of the eastward-migrating compressional system. Within this setting, transfer zones developed in a non-Andersonian mode in the hanging walls of the NW-SE–striking normal faults to separate differently stretched adjacent compartments (e.g., Gibbs, 1984). (2) As the extension progressed (late Quaternary; Fig. 14B), vigorous crustal thinning and erosion reduced the lithostatic load (σ_1), providing a new stress regime probably characterized by a vertical σ_2 axis (switch between σ_1 and σ_2) and horizontal σ_1 and σ_3. At this stage, the NW-SE–striking extensional faults became less effective, whereas the former shallow transfer zones switched to strike-slip crustal-scale faults. Both the preexisting NE-SW–striking and some newly generated N-S–striking strike-slip to transtensional faults responded to a horizontal σ_1 and propagated downward into the crust so as to reach the endogenic fluids accumulated at depth and offer them a viable pathway for surficial uprising and mixing with meteoric waters.

CONCLUSIONS

(1) Quaternary travertine deposition in the Albegna basin in central Italy reflects the interaction and feedbacks among hydrothermal activity, active tectonics, and paleoclimate within a region of positive geothermal anomaly. While hydrothermalism provided the fluids and the heat, tectonics controlled the location of faults, and paleoclimate modulated the abundance and elevation of groundwaters that buffered and mixed with the endogenic fluids.

(2) The reason for the southward and downward migration of the thermogene travertine depositional system remains to be explained. As such, the Albegna basin remains an interesting topic to be further studied for a better understanding of additional causes, e.g., eustatism, morphological molding, and groundwater-level changes as influenced by climate oscillations and endogenic fluid supply.

(3) The reconstructed spatio-temporal tectonic-hydrothermal evolution of the Albegna basin sheds light on the neotectonic and hydrothermal activity along many faults transverse to the Tyrrhenian margin, where, due to a change in the stress tensor induced by postorogenic crustal thinning, these originally shallow faults were reactivated and enhanced so as to propagate rupture downward into the crust and generate effective pathways for hydrothermal outflow.

ACKNOWLEDGMENTS

We thank C. Faccenna for fruitful discussions and G. Fellin for her help in the field and in the laboratory at ETH Zürich. The "Saturnia Travertini" company is acknowledged for kindly providing quarry access and logistic assistance. S. Kele was supported by the János Bolyai scholarship of the Hungarian Academy of Sciences and the Hungarian Scientific Research Fund (OTKA 101664). This manuscript benefited from comments and advice from S. Zanchetta and two anonymous reviewers. The editor (K. Stüwe) is acknowledged for the editorial handling.

REFERENCES CITED

Acocella, V., and Funiciello, R., 2002, Transverse structures and volcanic activity along the Tyrrhenian margin of central Italy: Bollettino della Società Geologica Italiana, v. 1, special issue, p. 739–747.

Acocella, V., and Funiciello, R., 2006, Transverse systems along the extensional Tyrrhenian margin of central Italy and their influence on volcanism: Tectonics, v. 25, p. TC2003, doi:10.1029/2005TC001845.

Acocella, V., and Rossetti, F., 2002, The role of extensional structures on pluton ascent and emplacement: The case of southern Tuscany (Italy): Tectonophysics, v. 354, p. 71–83, doi:10.1016/S0040-1951(02)00290-1.

Aiello, G., Marsella, E., and Sacchi, M., 2000, Quaternary structural evolution of Terracina and Gaeta basins (eastern Tyrrhenian margin, Italy): Rendiconti Fisica Accademia dei Lincei, v. 11, p. 41–58, doi:10.1007/BF02904595.

Altunel, E., and Hancock, P.L., 1993, Morphology and structural setting of Quaternary travertines at Pamukkale, Turkey: Geological Journal, v. 28, p. 335–346, doi:10.1002/gj.3350280312.

Altunel, E., and Karabacak, V., 2005, Determination of horizontal extension from fissure-ridge travertines: A case study from the Denizli Basin, southwestern Turkey: Geodinamica Acta, v. 18, no. 3–4, p. 333–342, doi:10.3166/ga.18.333-342.

Annunziatellis, A., Beaubien, S.E., Bigi, S., Ciotoli, G., Coltella, M., and Lombardi, S., 2008, Gas migration along fault systems and through the vadose zone in the Latera caldera (central Italy): Implications for CO_2 geological storage: International Journal of Greenhouse Gas Control, v. 2, p. 353–372, doi:10.1016/j.ijggc.2008.02.003.

Baillieux, P., Schill, E., Edel, J.B., and Mauri, G., 2013, Localization of temperature anomalies in the Upper Rhine Graben: Insights from geophysics and neotectonic activity: International Geology Review, v. 55, no. 14, p. 1744–1762, doi:10.1080/00206814.2013.794914.

Baldi, P., Ferrara, G.C., Masselli, L., and Pieretti, G., 1973, Hydrogeochemistry of the region between Monte Amiata and Rome: Geothermics, v. 2, p. 124–128, doi:10.1016/0375-6505(73)90020-5.

Baldi, P., Decandia, F.A., Lazzarotto, A., and Calamai, A., 1974, Studio geologico del sub-strato della copertura vulcanica Laziale nella zona dei laghi di Bolsena, Vico e Bracciano: Memorie della Società Geologica Italiana, v. 13, p. 575–606.

Barazzuoli, P., Capacci, F., Migliorini, J., and Rigati, R., 2013, Termalismo e travertini in Toscana meridionale, *in* Billi, A., De Filippis, L., and Ubertini, L., eds., Acque e Travertini: Rendiconti Online della Società Geologica Italiana, v. 27, p. 42–53, doi:10.3301/ROL.2013.19.

Barberi, F., Innocenti, F., and Ricci, C.A., 1971, Il magmatismo dell'Appennino Centro Settentrionale: Rendiconti della Società Italiana di Mineralogia e Petrologia, v. 27, p. 169–210.

Barberi, F., Buonasorte, G., Cioni, R., Fiordelisi, A., Foresi, L., Iaccarino, S., Laurenzi, M.A., Sbrana, A., Vernia, L., and Villa, I.M., 1994, Plio-Pleistocene geological evolution of the geothermal area of Tuscany and Latium: Memorie Descrittive della Carta Geologica Italiana, v. 49, p. 77–133.

Barchi, M., Minelli, G., and Pialli, G., 1998, The CROP-03 profile: A synthesis of results on deep structures of the Northern Apennines: Memorie della Societa Geologica Italiana, v. 52, p. 383–400.

Barilaro, F., Della Porta, G., and Capezzuoli, E., 2012, Depositional geometry and fabric types of hydrothermal travertine deposits (Albegna Valley, Tuscany, Italy): Rendiconti Online della Società Geologica Italiana, v. 21, p. 1024–1025.

Bartole, R., 1995, The North Tyrrhenian–Northern Apennines post-collisional system: Constraint for a geodynamic model: Terra Nova, v. 7, p. 7–30, doi:10.1111/j.1365-3121.1995.tb00664.x.

Batini, F., Brogi, A., Lazzarotto, A., Liotta, D., and Pandeli, E., 2003, Geological features of the Larderello-Travale and Monte Amiata geothermal areas (southern Tuscany, Italy): Episodes, v. 26, p. 239–244.

Bellani, S., Brogi, A., Lazzarotto, A., Liotta, D., and Ranalli, G., 2004, Heat flow, deep temperatures and extensional structures in the Larderello geothermal field (Italy). Constraints on geothermal fluid flow: Journal of Volcanology and Geothermal Research, v. 132, p. 15–29, doi:10.1016/S0377-0273(03)00418-9.

Berardi, G., Vignaroli, G., Billi, A., Rossetti, F., Soligo, M., Kele, S., Baykara, M.O., Bernasconi, S.M., Castorina, F., Tecce, F., and Shen, C.C., 2016, Growth of a Pleistocene giant carbonate vein and nearby thermogene travertine deposits at Semproniano, southern Tuscany, Italy: Estimate of CO_2 leakage: Tectonophysics, doi:10.1016/j.tecto.2016.04.014 (in press).

Bertani, R., 2005, World geothermal power generation in the period 2001–2005: Geothermics, v. 34, p. 651–690, doi:10.1016/j.geothermics.2005.09.005.

Bettelli, G., Bonazzi, U., Fazzini, P., Fontana, D., and Gasperi, G., 1990, Carta Geologica del Bacino del F. Albegna: Firenze, Italy, Istituto di Geologia dell'Universita di Modena, S.EL.CA, scale: 1:50,000.

Bibby, H.M., Caldwell, T.G., Davey, F.J., and Webb, T.H., 1995, Geophysical evidence on the structure of the Taupo volcanic zone and its hydrothermal circulation: Journal of Volcanology and Geothermal Research, v. 68, p. 29–58, doi:10.1016/0377-0273(95)00007-H.

Bigi, S., Beaubien, S.E., Ciotoli, G., D'Ambrogi, C., Doglioni, C., Ferrante, V., Lombardi, S., Milli, S., Orlando, L., Ruggiero, L., Tartarello, M.C., and Sacco, P., 2014, Mantle-derived CO_2 migration along active faults within an extensional basin margin (Fiumicino, Rome, Italy): Tectonophysics, v. 637, p. 137–149, doi:10.1016/j.tecto.2014.10.001.

Billi, A., and Tiberti, M.M., 2009, Possible causes of arc development in the Apennines, central Italy: Geological Society of America Bulletin, v. 121, p. 1409–1420, doi:10.1130/B26335.1.

Billi, A., Bosi, V., and De Meo, A., 1997, Caratterizzazione strutturale del rilievo del Monte Massico nell'ambito dell'evoluzione quaternaria delle depressioni costiere dei fiumi Garigliano e Volturno (Campania settentrionale): Il Quaternario: Italian Journal of Quaternary Sciences, v. 10, p. 15–26.

Billi, A., Tiberti, M.M., Cavinato, G.P., Cosentino, D., Di Luzio, E., Keller, J.V.A., Kluth, C., Orlando, L., Parotto, M., Praturlon, A., Romanelli, M., Storti, F., and Wardell, N., 2006, First results from the CROP-11 deep seismic profile, central Apennines, Italy: Evidence of mid-crustal folding: Journal of the Geological Society, London, v. 163, p. 583–586, doi:10.1144/0016-764920-002.

Billi, A., Valle, A., Brilli, M., Faccenna, C., and Funiciello, R., 2007, Fracture-controlled fluid circulation and dissolutional weathering in sinkhole-prone carbonate rocks from central Italy: Journal of Structural Geology, v. 29, p. 385–395, doi:10.1016/j.jsg.2006.09.008.

Boccaletti, M., Calamita, F., Deiana, G., Gelati, R., Massari, F., Moratti, G., and Ricci Lucchi, F., 1990, Migrating foredeep-thrust belt systems in the Northern Apennines and southern Alps: Palaeogeography, Palaeoclimatology, Palaeoecology, v. 77, p. 3–14, doi:10.1016/0031-0182(90)90095-O.

Boccaletti, M., Gianelli, G., and Sani, F., 1997, Tectonic regime, granite emplacement and crustal structure in the inner zone of the Northern Apennines (Tuscany, Italy): A new hypothesis: Tectonophysics, v. 270, p. 127–143, doi:10.1016/S0040-1951(96)00177-1.

Bonazzi, U., Fazzini, P., and Gasperi, G., 1992, Note alla carta geologica del Bacino del Fiume Albegna: Bollettino della Società Geologica Italiana, v. 111, p. 341–354.

Bonciani, F., Callegari, I., Conti, P., Cornamusini, G., and Carmignani, L., 2005, Neogene post-collisional evolution of the internal Northern Apennines: Insights from the upper Fiora and Albegna valleys (Mt. Amiata geothermal area, southern Tuscany): Bollettino della Società Geologica Italiana, v. 3, special issue, p. 103–118.

Bonini, M., Sani, F., Stucchi, E.M., Moratti, G., Benvenuti, M., Menanno, G., and Tanini, C., 2014, Late Miocene shortening of the Northern Apennines back-arc: Journal of Geodynamics, v. 74, p. 1–31, doi:10.1016/j.jog.2013.11.002.

Bosi, C., Messina, P., Rosati, M., and Sposato, A., 1996, Età dei travertini della Toscana meridionale e relative implicazioni neotettoniche: Memorie della Società Geologica Italiana, v. 51, p. 293–304.

Bossio, A., Costantini, A., Lazzarotto, A., Liotta, D., Mazzanti, R., Mazzei, R., Salvatorini, G., and Sandrelli, F., 1993, Rassegna delle conoscenze sulla stratigrafiad el Neautoctono Toscano: Memorie della Società Geologica Italiana, v. 49, p. 17–98.

Bossio, A., Foresi, L.M., Mazzei, R., Salvatorini, G., Sandrelli, F., Bilotti, M., Colli, A., and Rossetto, R., 2003, Geology and stratigraphy of the southern sector of the Neogene Albegna River Basin (Grosseto, Tuscany, Italy): Geologica Romana, v. 37, p. 165–173.

Breitenbach, S.F.M., and Bernasconi, S.M., 2011, Carbon and oxygen isotope analysis of small carbonate samples (20 to 100 µg) with a GasBench II preparation device: Rapid Communications in Mass Spectrometry, v. 25, p. 1910–1914, doi:10.1002/rcm.5052.

Brogi, A., 2004a, Miocene extension in the inner Northern Apennines: The Tuscan nappe megaboudins in the Mt. Amiata geothermal area and their influence on Neogene sedimentation: Bollettino della Società Geologica Italiana, v. 123, p. 513–529.

Brogi, A., 2004b, Faults linkage, damage rocks and hydrothermal fluid circulation: Tectonic interpretation of the Rapolano Terme travertines (southern Tuscany, Italy) in the context of the Northern Apennines Neogene–Quaternary extension: Eclogae Geologicae Helvetiae, v. 97, p. 307–320, doi:10.1007/s00015-004-1134-5.

Brogi, A., 2008, The structure of the Monte Amiata volcano-geothermal area (Northern Apennines, Italy): Neogene–Quaternary compression versus extension: International Journal of Earth Sciences, v. 97, p. 677–703, doi:10.1007/s00531-007-0191-1.

Brogi, A., 2011, Bowl-shaped basin related to low-angle detachment during continental extension: The case of the controversial Neogene Siena Basin (central Italy, Northern Apennines): Tectonophysics, v. 499, p. 54–76, doi:10.1016/j.tecto.2010.12.005.

Brogi, A., and Capezzuoli, E., 2009, Travertine deposition and faulting: The fault-related travertine fissure-ridge at Terme S. Giovanni, Rapolano Terme (Italy): International Journal of Earth Sciences, v. 98, p. 931–947, doi:10.1007/s00531-007-0290-z.

Brogi, A., and Fabbrini, L., 2009, Extensional and strike-slip tectonics across the Monte Amiata–Monte Cetona transect (Northern Apennines, Italy) and seismotectonic implications: Tectonophysics, v. 476, p. 195–209, doi:10.1016/j.tecto.2009.02.020.

Brogi, A., and Liotta, D., 2008, Highly extended terrains, lateral segmentation of the substratum, and basin development: The middle-late Miocene Radicondoli Basin (inner Northern Apennines, Italy): Tectonics, v. 27, p. TC5002, doi:10.1029/2007TC002188.

Brogi, A., Capezzuoli, E., Aquè, R., Branca, M., and Voltaggio, M., 2010a, Studying travertines for neotectonics investigations: Middle–Late Pleistocene syn-tectonic travertine deposition at Serre di Rapolano (Northern Apennines, Italy): International Journal of Earth Sciences, v. 99, p. 1383–1398, doi:10.1007/s00531-009-0456-y.

Brogi, A., Liotta, D., Meccheri, M., and Fabbrini, L., 2010b, Transtensional shear zones controlling volcanic eruptions: The middle Pleistocene Mt. Amiata volcano (inner Northern Apennines, Italy): Terra Nova, v. 22, p. 137–146, doi:10.1111/j.1365-3121.2010.00927.x.

Brogi, A., Capezzuoli, E., Buracchi, E., and Branca, M., 2012, Tectonic control on travertine and calcareous tufa deposition in a low-temperature geothermal system (Sarteano, central Italy): Journal of the Geological Society, London, v. 169, p. 461–476, doi:10.1144/0016-76492011-137.

Brogi, A., Fidolini, F., and Liotta, D., 2013, Tectonic and sedimentary evolution of the Upper Valdarno Basin: New insights from the lacustrine S. Barbara Basin: Italian Journal of Geosciences, v. 132, no. 1, p. 81–97, doi:10.3301/IJG.2012.08.

Brogi, A., Capezzuoli, E., Martini, I., Picozzi, M., and Sandrelli, F., 2014, Late Quaternary tectonics in the inner Northern Apennines (Siena Basin, southern Tuscany, Italy) and their seismotectonic implication: Journal of Geodynamics, v. 76, p. 25–45, doi:10.1016/j.jog.2014.03.001.

Brogi, A., Capezzuoli, E., Liotta, D., and Meccheri, M., 2015, The Tuscan nappe structures in the Monte Amiata geothermal area (central Italy): A review: Italian Journal of Geosciences, v. 134, p. 219–236, doi:10.3301/IJG.2014.55.

Browne, P.R.L., 1978, Hydrothermal alteration in active geothermal fields: Annual Review of Earth and Planetary Sciences, v. 6, p. 229–248, doi:10.1146/annurev.ea.06.050178.001305.

Buonasorte, G., Cataldi, R., Ceccarelli, A., Costantini, A., D'Offizi, S., Lazzarotto, A., Ridolfi, A., Baldi, P., Barelli, A., Bertini, G., Bertrami, R., Calamai, A., Cameli, G., Corsi, R., D'Acquino, C., Fiordelisi, A., Gezzo, A., and Lovari, F., 1988, Ricerca ed esplorazione nell'area geotermica di Torre Alfina (Lazio–Umbria): Bollettino della Società Geologica Italiana, v. 107, p. 265–337.

Buttinelli, M., Chiarabba, C., Anselmi, M., Bianchi, I., De Rita, D., and Quattrocchi, F., 2014, Crustal structure of northern Latium (central Italy) from receiver functions analysis: New evidences of a post-collisional back-arc margin evolution: Tectonophysics, v. 621, p. 148–158.

Cadoux, A., and Pinti, D.L., 2009, Hybrid character and pre-eruptive events of Mt Amiata volcano (Italy) inferred from geochronological, petro-geochemical and isotopic data: Journal of Volcanology and Geothermal Research, v. 179, p. 169–190, doi:10.1016/j.jvolgeores.2008.10.018.

Caine, J.S., Evans, J.P., and Forster, C.B., 1996, Fault zone architecture and permeability structure: Geology, v. 24, p. 1025–1028, doi:10.1130/0091-7613(1996)024<1025:FZAAPS>2.3.CO;2.

Capezzuoli, E., 2013, Il patrimonio di travertini e calcareous tufa in Toscana, *in* Billi, A., De Filippis, L., and Ubertini, L., eds., Acque e Travertini: Rendiconti Online della Società Geologica Italiana, v. 27, p. 31–41, doi:10.3301/ROL.2013.18.

Carmignani, L., Decandia, F.A., Fantozzi, P.L., Lazzarotto, A., Liotta, D., and Meccheri, M., 1994, Tertiary extensional tectonics in Tuscany (Northern Apennines, Italy): Tectonophysics, v. 238, p. 295–315, doi:10.1016/0040-1951(94)90061-2.

Carmignani, L., Conti, P., Cornamusini, G., and Pirro, A., 2013, Geological map of Tuscany (Italy): Journal of Maps, v. 9, no. 4, p. 487–497, doi:10.1080/17445647.2013.820154.

Cas, R.A.F., Giordano, G., Esposito, A., Balsamo, F., and Lo Mastro S., 2011, Hydrothermal breccia textures and processes: Lisca Bianca Islet, Panarea, Eolian Islands, Italy: Economic Geology and the Bulletin of the Society of Economic Geologists, v. 106, p. 437–450, doi:10.2113/econgeo.106.3.437.

Cavinato, G.P., and De Celles, P.G., 1999, Extensional basins in the tectonically bimodal central Apennines fold-thrust belt, Italy: Response to corner flow above a subducting slab in retrograde motion: Geology, v. 27, p. 955–958, doi:10.1130/0091-7613(1999)027<0955:EBITTB>2.3.CO;2.

Cerrina Feroni, A., Bonini, M., Martinelli, P., Moratti, G., Sani, F., Montanari, D., and Del Ventisette, C., 2006, Lithological control on thrust-related deformation in the Sassa-Guardistallo Basin (Northern Apennines hinterland, Italy): Basin Research, v. 18, p. 301–321, doi:10.1111/j.1365-2117.2006.00295.x.

Chafetz, H.S., and Guidry, S.A., 2003, Deposition and diagenesis of Mammoth Hot Springs travertine, Yellowstone National Park, Wyoming, U.S.A.: Canadian Journal of Earth Sciences, v. 40, p. 1515–1529, doi:10.1139/e03-051.

Chiarabba, C., Amato, A., and Fiordelisi, A., 1995, Upper crustal tomographic images of the Amiata–Vulsini geothermal region, central Italy: Journal of Geophysical Research, v. 100, p. 4053–4066.

Chiocchini, U., Castaldi, F., Barbieri, M., and Eulilli, V., 2010, A stratigraphic and geophysical approach to studying the deep circulating groundwater and thermal springs, and their recharge areas, in Cimini Mountains–Viterbo area, central Italy: Hydrogeology Journal, v. 18, p. 1319–1341, doi:10.1007/s10040-010-0601-5.

Chiodini, G., Frondini, F., and Ponziani, F., 1995, Deep structures and carbon dioxide degassing in central Italy: Geothermics, v. 24, p. 81–94, doi:10.1016/0375-6505(94)00023-6.

Cifelli, F., Minelli, L., Rossetti, F., Urru, G., and Mattei, M., 2012, The emplacement of the late Miocene Monte Capanne intrusion (Elba Island, central Italy): Constraints from magnetic fabric analyses: International Journal of Earth Sciences, v. 101, p. 787–802, doi:10.1007/s00531-011-0701-z.

Cipollari, P., and Cosentino, D., 1995, Miocene unconformities in the central Apennines: Geodynamic significance and sedimentary basin evolution: Tectonophysics, v. 252, p. 375–389, doi:10.1016/0040-1951(95)00088-7.

Collettini, C., De Paola, N., Holdsworth, R.E., and Barchi, M.R., 2006, The development and behavior of low-angle normal faults during Cenozoic asymmetric extension in the Northern Apennines, Italy: Journal of Structural Geology, v. 28, p. 333–352, doi:10.1016/j.jsg.2005.10.003.

Conticelli, S., Boari, E., Burlamacchi, L., Cifelli, F., Moscardi, F., Laurenzi, M.A., Ferrari Pedraglio, L., Francalanci, L., Benvenuti, M.G., Braschi, E., and Manetti, P., 2015, Geochemistry and Sr-Nd-Pb isotopes of Monte Amiata volcano, central Italy: Evidence for magma mixing between high-K calc-alkaline and leucititic mantle-derived magmas: Italian Journal of Geosciences, v. 134, p. 266–290, doi:10.3301/IJG.2015.12.

Corniello, A., Cardellicchio, N., Cavuoto, G., Cuoco, E., Ducci, D., Minissale, A., Mussi, M., Petruccione, E., Pelosi, N., Rizzo, E., Polemico, M., Tamburino, S., Tedesco, D., Tiano, P., and Iorio, M., 2015, Hydrogeological characterization of a geothermal system: The case of the thermo-mineral area of Mondragone (Campania, Italy): International Journal of Environmental of Research, v. 9, p. 523–534.

Corrado, S., Aldega, L., Celano, A.S., De Benedetti, A.A., and Giordano, G., 2014, Cap rock efficiency and fluid circulation of natural hydrothermal systems by means of XRD on

clay minerals (Sutri, northern Latium, Italy): Geothermics, v. 50, p. 180–188, doi:10.1016/j.geothermics.2013.09.011.
Costantini, A., Ghezzo, C., and Lazzarotto, A., 1984, Carta Geologica dell'Area Geotermica di Torre Alfina (Prov. Di Siena-Viterbo-Terni): Firenze, Italy, ENEL (Ente nazionale per l'energia elettrica), Unità Nazionale Geotermica–Pisa, Cartografia S.EL.C.A, scale 1:25,000.
Cox, S.F., Knackstedt, M.A., and Braun, J., 2001, Principles of structural controls on permeability and fluid flow in hydrothermal systems: Reviews in Economic Geology, v. 14, p. 1–24.
Croci, A., Della Porta, G., and Capezzuoli, E., 2016, Depositional architecture of a mixed travertine-terrigenous system in a fault-controlled continental extensional basin (Messinian, southern Tuscany, central Italy): Sedimentary Geology, v. 332, p. 13–39, doi:10.1016/j.sedgeo.2015.11.007.
Crossey, L.C., Karlstrom, K.E., Dorsey, R., Pearce, J., Wan, E., Beard, L.S., Asmerom, Y., Polyak, V., Crow, R.S., Cohen, A., Bright, J., and Pecha, M.E., 2015, Importance of groundwater in propagating downward integration of the 6–5 Ma Colorado River system: Geochemistry of springs, travertines, and lacustrine carbonates of the Grand Canyon region over the past 12 Ma: Geosphere, v. 11, p. 660–682, doi:10.1130/GES01073.1.
Crossey, L.J., and Karlstrom, K.E., 2012, Travertines and travertine springs in eastern Grand Canyon: What they tell us about groundwater, paleoclimate, and incision of Grand Canyon, *in* Timmons, J.M., and Karlstrom, K.E., eds., Grand Canyon Geology: Two Billion Years of Earth's History: Geological Society of America Special Paper 489, p. 131–143, doi:10.1130/2012.2489(09).
Crossey, L.J., Fischer, T.P., Patchett, P.J., Karlstrom, K.E., Hilton, D.R., Newell, D.L., Huntoon, P., Reynolds, A.C., and de Leeuw, G.A.M., 2006, Dissected hydrologic system at the Grand Canyon: Interaction between deeply derived fluids and plateau aquifer waters in modern springs and travertine: Geology, v. 34, p. 25–28, doi:10.1130/G22057.1.
Curewitz, D., and Karson, J.A., 1997, Structural settings of hydrothermal outflow: Fracture permeability maintained by fault propagation and interaction: Journal of Volcanology and Geothermal Research, v. 79, p. 149–168, doi:10.1016/S0377-0273(97)00027-9.
De Filippis, L., and Billi, A., 2012, Morphotectonics of fissure ridge travertines from geothermal areas of Mammoth Hot Springs (Wyoming) and Bridgeport (California): Tectonophysics, v. 548–549, p. 34–48, doi:10.1016/j.tecto.2012.04.017.
De Filippis, L., Faccenna, C., Billi, A., Anzalone, E., Brilli, M., Soligo, M., and Tuccimei, P., 2013a, Plateau versus fissure ridge travertines from Quaternary geothermal springs of Italy and Turkey: Interactions and feedbacks between fluid discharge, paleoclimate, and tectonics: Earth-Science Reviews, v. 123, p. 35–52, doi:10.1016/j.earscirev.2013.04.004.
De Filippis, L., Anzalone, E., Billi, A., Faccenna, C., Poncia, P.P., and Sella, P., 2013b, The origin and growth of a recently-active fissure ridge travertine over a seismic fault, Tivoli, Italy: Geomorphology, v. 195, p. 13–26, doi:10.1016/j.geomorph.2013.04.019.
Della Vedova, B., Bellani, S., Pellis, G., and Squarci, P., 2001, Deep temperatures and surface heat flow distribution, *in* Vai, G.B., and Martini, I.P., eds., Anatomy of an Orogen: The Apennines and Adjacent Mediterranean Basins: Dordrecht, Netherlands, Kluwer Academic Publisher, p. 65–76.
Dewey, J.F., Helman, M.L., Knott, S.D., Turco, E., and Hutton, D.H.W., 1989, Kinematics of the western Mediterranean, *in* Coward, M.P., Dietrich, D., and Park, R.G., eds., Alpine Tectonics: Geological Society, London, Special Publication 45, p. 265–283, doi:10.1144/GSL.SP.1989.045.01.15.
Dilsiz, C., 2006, Conceptual hydrodynamic model of the Pamukkale hydrothermal field, southwestern Turkey, based on hydrochemical and isotopic data: Hydrogeology Journal, v. 14, p. 562–572, doi:10.1007/s10040-005-0001-4.
Dini, A., Granelli, G., Puxeddu, M., and Ruggieri, G., 2005, Origin and evolution of Pliocene–Pleistocene granites from the Larderello geothermal field (Tuscan magmatic province, Italy): Lithos, v. 81, p. 1–31, doi:10.1016/j.lithos.2004.09.002.
Doglioni, C., 1991, A proposal for the kinematic modelling of W-dipping subductions: Possible applications to the Tyrrhenian-Apennines system: Terra Nova, v. 3, p. 423–434, doi:10.1111/j.1365-3121.1991.tb00172.x.
Dramis, F., Materazzi, M., and Cilla, G., 1999, Influence of climatic changes on freshwater travertine deposition: A new hypothesis: Physics and Chemistry of the Earth, ser. A, Solid Earth and Geodesy, v. 24, p. 893–897, doi:10.1016/S1464-1895(99)00132-5.
Duchi, V., Minissale, A., Paolieri, M., Prati, F., and Valori, A., 1992, Chemical relationship between discharging fluids in the Siena-Radicofani graben and the deep fluids produced by the geothermal fields of the Mt. Amiata, Torre Alfina and Latera (central Italy): Geothermics, v. 21, p. 401–413, doi:10.1016/0375-6505(92)90089-R.
Edwards, R.L., Chen, J.H., and Wasserburg, G.J., 1987, ^{238}U-^{234}U-^{230}Th systematics and the precise measurement of time over the last 500,000 years: Earth and Planetary Science Letters, v. 81, p. 175–192, doi:10.1016/0012-821X(87)90154-3.
Engin, B., Güven, O., and Köksal, F., 1999, Electron spin resonance age determination of a travertine sample from the southwestern part of Turkey: Applied Radiation and Isotopes, v. 51, p. 689–699, doi:10.1016/S0969-8043(99)00090-1.
Faccenna, C., Funiciello, R., Bruni, A., Mattei, M., and Sagnotti, L., 1994, Evolution of a transfer-related basin: The Ardea basin (Latium, central Italy): Basin Research, v. 6, p. 35–46, doi:10.1111/j.1365-2117.1994.tb00073.x.
Faccenna, C., Mattei, M., Funiciello, R., and Jolivet, L., 1997, Styles of back-arc extension in the central Mediterranean: Terra Nova, v. 9, p. 126–130, doi:10.1046/j.1365-3121.1997.d01-12.x.
Faccenna, C., Piromallo, C., Crespo-Blanc, A., Jolivet, L., and Rossetti, F., 2004, Lateral slab deformation and the origin of the western Mediterranean arcs: Tectonics, v. 23, p. TC1012, doi:10.1029/2002TC001488.
Faccenna, C., Soligo, M., Billi, A., De Filippis, L., Funiciello, R., Rossetti, C., and Tuccimei, P., 2008, Late Pleistocene depositional cycles of the Lapis Tiburtinus travertine (Tivoli, central Italy): Possible influence of climate and fault activity: Global and Planetary Change, v. 63, p. 299–308, doi:10.1016/j.gloplacha.2008.06.006.
Farina, F., Dini, A., Innocenti, F., Rocchi, S., and Westerman, D.S., 2010, Rapid incremental assembly of the Monte Capanne pluton (Elba Island, Tuscany) by downward stacking of magma sheets: Geological Society of America Bulletin, v. 122, p. 1463–1479, doi:10.1130/B30112.1.
Fouke, B.W., Farmer, J.D., Des Marais, D.J., Pratt, L., Sturchio, N.C., Burns, P.C., and Discipulo, M.K., 2000, Depositional facies and aqueous-solid geochemistry of travertine-depositing hot spring (Angel Terrace, Mammoth Hot Spring, Yellowstone National Park, U.S.A.): Journal of Sedimentary Research, v. 70, no. 3, p. 565–585, doi:10.1306/2DC40929-0E47-11D7-8643000102C1865D.
Frank, N., Braum, M., Hambach, U., Mangini, A., and Wagner, G., 2000, Warm period growth of travertine during the last interglaciation in southern Germany: Quaternary Research, v. 54, p. 38–48, doi:10.1006/qres.2000.2135.
Frepoli, A.F., Marra, C., Maggi, A., Marchetti, A., Nardi, N., Pagliuca, M., and Pirro, M., 2010, Seismicity, seismogenic structures, and crustal stress fields in the greater Rome area (central Italy): Journal of Geophysical Research, v. 115, p. B12303, doi:10.1029/2009JB006322.
Frery, E., Gratier, J.P., Ellouz-Zimmerman, N., Loiselet, C., Braun, J., Deschamps, P., Blamart, D., Hamelin, B., and Swennen, R., 2015, Evolution of fault permeability during episodic fluid circulation: Evidence for the effects of fluid–rock interactions from travertine studies (Utah–USA): Tectonophysics, v. 651–652, p. 121–137, doi:10.1016/j.tecto.2015.03.018.
Friedman, I., 1970, Some investigation of the deposition of travertine from hot springs: I. The isotopic chemistry of a travertine-depositing spring: Geochimica et Cosmochimica Acta, v. 34, p. 1303–1315, doi:10.1016/0016-7037(70)90043-8.
Gandin, A., and Capezzuoli, E., 2008, Travertine versus calcareous tufa: Distinctive petrologic features and related stable isotopes signature: Il Quaternario: Italian Journal of Quaternary Science, v. 21, p. 125–136.
Gasparini, C., Di Maro, R., Pagliuca, N., Pirro, M., and Marchetti, A., 2002, Recent seismicity of the "Acque Albule" travertine basin: Annals of Geophysics, v. 45, p. 537–550.
Gelmini, R., Mantovani, P., and Mucchi, A.M., 1967, La serie a facies Toscana del Fiume Albegna presso Semproniano (già Semprugnano–Grosseto): Memorie della Società Geologica Italiana, v. 6, p. 359–378.
Gianelli, G., Manzella, A., and Puxeddu, M., 1997, Crustal models of the geothermal areas of southern Tuscany (Italy): Tectonophysics, v. 281, p. 221–239, doi:10.1016/S0040-1951(97)00101-7.
Gibbs, A.D., 1984, Structural evolution of extensional basin margins: Journal of the Geological Society, London, v. 141, p. 609–620, doi:10.1144/gsjgs.141.4.0609.
Gonfiantini, R., Panichi, C., and Tongiorgi, E., 1968, Isotopic disequilibrium in travertine deposition: Earth and Planetary Science Letters, v. 5, p. 55–58, doi:10.1016/S0012-821X(68)80012-3.
Guastaldi, E., Graziano, L., Liali, G., Nunzio, F., Brogna, A., and Barbagli, A., 2014, Intrinsic vulnerability assessment of Saturnia thermal aquifer by means of three parametric methods: SINTACS, GODS and COP: Environmental Earth Sciences, v. 72, p. 2861–2878, doi:10.1007/s12665-014-3191-z.
Gudmundsson, A., 2011, Rock Fractures in Geological Processes: Cambridge, UK, Cambridge University Press, 592 p.
Guo, L., Andrews, J., Riding, R., Dennis, P., and Dresser, Q., 1996, Possible microbial effects on stable carbon isotopes in hot travertine: Journal of Sedimentary Research, v. 66, p. 468–473, doi:10.1306/D4268379-2B26-11D7-8648000102C1865D.
Hancock, P.L., Chalmers, R.M.L., Altunel, E., and Çakir, Z., 1999, Travitonics: Using travertines in active fault studies: Journal of Structural Geology, v. 21, p. 903–916, doi:10.1016/S0191-8141(99)00061-9.
Ingrassia, M., Martorelli, E., Bosman, A., Macelloni, L., Sposato, A., and Chiocci, F.L., 2015, The Zannone giant pockmark: First evidence of a giant complex seeping structure in shallow-water, central Mediterranean Sea, Italy: Marine Geology, v. 363, p. 38–51, doi:10.1016/j.margeo.2015.02.005.
Innocenti, F., Serri, G., Ferrara, G., Manetti, P., and Tonarini, S., 1992, Genesis and classification of the rocks of the Tuscan magmatic province: Thirty years after the Marinelli's model: Acta Vulcanologica, v. 2, p. 247–265.
Ivanovich, M., and Harmon, R.S., 1992, Uranium-Series Disequilibrium: Applications to Earth, Marine, and Environmental Sciences: Oxford, UK Clarendon Press, 910 p.
Jacobacci, A., Martelli, G., and Nappi, G., 1967, Note Illustrative della Carta Geologica d'Italia, Foglio 129, S. Fiora: Roma, La Litografia, scale 1:100,000.
Jolivet, L., Faccenna, C., Goffé, B., Mattei, M., Rossetti, F., Brunet, C., Storti, F., Funiciello, R., Cadet, J.P., D'Agostino, N., and Parra, T., 1998, Midcrustal shear zones in post-orogenic extension: Example from the northern Tyrrhenian Sea (Italy): Journal of Geophysical Research, v. 103, p. 12,123–12,160, doi:10.1029/97JB03616.
Kampman, N., Burnside, N.M., Shipton, Z.K., Chapman, H.J., Nicholl, J.A., Ellam, R.M., and Bickle, M.J., 2012, Pulses of carbon dioxide emissions from intracrustal faults following climatic warming: Nature Geoscience, v. 5, p. 352–358, doi:10.1038/ngeo1451.
Karlstrom, K.E., Crossey, L.J., Hilton, D.R., and Barry, P.H., 2013, Mantle ^{3}He and CO_2 degassing in carbonic and geothermal springs of Colorado and implications for neotectonics of the Rocky Mountains: Geology, v. 41, p. 495–498, doi:10.1130/G34007.1.
Kele, S., Vaselli, O., Szabó, C., and Minissale, A., 2003, Stable isotope geochemistry of Pleistocene travertine from Budakalász (Buda Mts, Hungary): Acta Geologica Hungarica, v. 46, no. 2, p. 161–175, doi:10.1556/AGeol.46.2003.2.4.
Kele, S., Özkul, M., Fórizs, I., Gökgöz, A., Baykara, M.O., and Alçiçek, M.C., 2011, Stable isotope geochemical study of Pamukkale travertines: New evidences of low-temperature non-equilibrium calcite-water fractionation: Sedimentary Geology, v. 238, p. 191–212, doi:10.1016/j.sedgeo.2011.04.015.
Kele, S., Breitenbach, S.F.M., Capezzuoli, E., Nele Meckler, A., Ziegler, M., Millan, I.M., Kluge, T., Deák, J., Hanselmann, K., John, C.M., Yan, H., Liu, Z., and Bernasconi, S.M., 2015, Temperature dependence of oxygen- and clumped isotope fractionation in carbonates: A study of travertines and tufas in the 6–95°C temperature range: Geochimica et Cosmochimica Acta, v. 168, p. 172–192, doi:10.1016/j.gca.2015.06.032.

Keller, J.V.A., Minelli, G., and Pialli, G., 1994, Anatomy of a late orogenic extension: The Northern Apennines case: Tectonophysics, v. 238, p. 275–294, doi.org/10.1016/0040-1951(94)90060-4.

Laurenzi, M.A., Braschi, E., Casalini, M., and Conticelli, S., 2015, New ^{40}Ar-^{39}Ar dating and revision of the geochronology of the Monte Amiata volcano, central Italy: Italian Journal of Geosciences, v. 134, p. 255–265, doi:10.3301/IJG.2015.11.

Lavecchia, G., Brozzetti, F., Barchi, M., Menichetti, M., and Keller, J.V.A., 1994, Seismotectonic zoning in east-central Italy deduced from an analysis of the Neogene to present deformations and related stress fields: Geological Society of America Bulletin, v. 106, p. 1107–1120, doi:10.1130/0016-7606(1994)106<1107:SZIECI>2.3.CO;2.

Lebatard, A.E., Alçiçek, A.C., Rochette, P., Khatib, S., Vialet, A., Boulbes, N., Bourlès, D.L., Demory, F., Guipert, G., Mayda, S., Titov, V.V., Vidal, L., and de Lumley, H., 2014, Dating the *Homo erectus* bearing travertine from Kocabas (Denizli, Turkey) at least 1.1 Ma: Earth and Planetary Science Letters, v. 390, p. 8–18, doi:10.1016/j.epsl.2013.12.031.

Liotta, D., 1991, The Arbia–Val Marecchia Line, Northern Apennines: Eclogae Geologicae Helvetiae, v. 84, no. 2, p. 413–430.

Liotta, D., 1994, Structural features of the Radicofani Basin along the Piancastagnaio (Mt. Amiata)–S. Casciano dei Bagni (Mt. Cetona) cross section: Memorie della Società Geologica Italiana, v. 48, p. 401–408.

Liotta, D., Ruggieri, G., Brogi, A., Fulignati, P., Dini, A., and Cardini, I., 2010, Migration of geothermal fluids in extensional terrains: The ore deposits of the Boccheggiano-Montieri area (southern Tuscany, Italy): International Journal of Earth Sciences, v. 99, p. 623–644, doi:10.1007/s00531-008-0411-3.

Liotta, D., Brogi, A., Meccheri, M., Dini, A., Bianco, C., and Ruggieri, G., 2015, Coexistence of low-angle normal and high-angle strike- to oblique-slip faults during late Miocene mineralization in eastern Elba Island (Italy): Tectonophysics, v. 660, p. 17–34, doi:10.1016/j.tecto.2015.06.025.

Locardi, E., and Nicolich, R., 1988, Geodinamica del Tirreno e dell'Appennino centro-meridionale: La nuova carta della Moho: Memorie della Società Geologica Italiana, v. 41, p. 121–140.

Ludwig, K.R., 2003, Isoplot/Ex Version 3.00, A Geochronological Toolkit for Microsoft Excel: Berkeley Geochronology Center Special Publication 4, 73 p.

Luque, J.A., and Julià, R., 2007, U/Th dating of Quaternary travertines at the middle Llobregat River (NE Iberian Peninsula, northwestern Mediterranean). Correlation with sea-level changes: Geologica Acta, v. 5, p. 109–117.

Malinverno, A., and Ryan, W., 1986, Extension in the Tyrrhenian Sea and shortening in the Apennines as result of arc migration driven by sinking of the lithosphere: Tectonics, v. 5, p. 227–245, doi:10.1029/TC005i002p00227.

Manfra, L., Masi, U., and Turi, B., 1974, Effetti isotopici nella diagenesi dei travertini: Geologica Romana, v. 13, p. 147–155.

Marinelli, G., Barberi, F., and Cioni, R., 1993, Sollevamenti neogenici e intrusioni acide della Toscana e del Lazio settentrionale: Memorie della Società Geologica Italiana, v. 49, p. 279–288.

Marroni, M., Moratti, G., Costantini, A., Conticelli, S., Benvenuti, M.G., Pandolfi, L., Bonini, M., Cornamusini, G., and Laurenzi, M.A., 2015, Geology of the Monte Amiata region, southern Tuscany, central Italy: Italian Journal of Geosciences, v. 134, p. 171–199, doi:10.3301/IJG.2015.13.

Martelli, L., Moratti, G., and Sani, F., 1989, Analisi strutturale dei travertini della Toscana meridionale (Valle dell'Albegna): Bollettino della Società Geologica Italiana, v. 108, p. 197–205.

Martini, I.P., and Sagri, M., 1993, Tectono-sedimentary characteristics of late Miocene–Quaternary extensional basins of the Northern Apennines, Italy: Earth-Science Reviews, v. 34, p. 197–233, doi:10.1016/0012-8252(93)90034-5.

Martini, I.P., Sagri, M., and Colella, A., 2001, Neogene–Quaternary basins of the inner Apennines and Calabrian arc, *in* Vai, G.B., and Martini, I.P., eds., Anatomy of an Orogen: The Apennines and Adjacent Mediterranean Basins: Dordrecht, Netherlands, Kluwer Academic Publisher, p. 375–400.

Massoli, D., Koyi, H.A., and Barchi, M.R., 2006, Structural evolution of a fold and thrust belt generated by multiple décollements: Analogue models and natural examples from the Northern Apennines (Italy): Journal of Structural Geology, v. 28, p. 185–199, doi:10.1016/j.jsg.2005.11.002.

Mazzini, A., Etiope, G., and Svensen, H., 2012, A new hydrothermal scenario for the 2006 Lusi eruption, Indonesia. Insights from gas geochemistry: Earth and Planetary Science Letters, v. 317–318, p. 305–318, doi:10.1016/j.epsl.2011.11.016.

Minissale, A., 2004, Origin, transport and discharge of CO_2 in central Italy: Earth-Science Reviews, v. 66, p. 89–141, doi:10.1016/j.earscirev.2003.09.001.

Musumeci, G., and Vaselli, L., 2012, Neogene deformation and granite emplacement in the metamorphic units of Northern Apennines (Italy): Insights from mylonitic marbles in the Porto Azzurro pluton contact aureole (Elba Island): Geosphere, v. 8, p. 470–490, doi:10.1130/GES00665.1.

Nappi, G., Renzulli, A., Santi, P., and Gillot, P.Y., 1995, Geological evolution and geochronology of the Vulsini volcano district (central Italy): Bollettino della Società Geologica Italiana, v. 114, p. 599–613.

Newell, D.L., Crossey, L.J., Karlstrom, K.E., Fischer, T.P., and Hilton, D.R., 2005, Continental-scale links between the mantle and groundwater systems of the western United States: Evidence from travertine springs and regional He isotope data: GSA Today, v. 15, no. 12, doi:10.1130/1052-5173(2005)015[4:CSLBTM]2.0.CO;2.

Özkul, M., Kele, S., Gökgöz, A., Shen, C.C., Jones, B., Baykara, M.O., Fórizs, I., Nemeth, T., Chang, Y.-W., and Alçiçek, M.C., 2013, Comparison of the Quaternary travertine sites in the Denizli extensional basin based on their depositional and geochemical data: Sedimentary Geology, v. 294, p. 179–204, doi:10.1016/j.sedgeo.2013.05.018.

Pascucci, V., Costantini, A., Martini, I.P., and Dringoli, R., 2006, Tectono-sedimentary analysis of a complex, extensional, Neogene basin formed on thrust-faulted, Northern Apennines hinterland: Radicofani Basin, Italy: Sedimentary Geology, v. 183, no. 1–2, p. 71–97, doi:10.1016/j.sedgeo.2005.09.009.

Patacca, E., Sartori, R., and Scandone, P., 1990, Tyrrhenian basin and Apenninic arcs: Kinematic relation since late Tortonian times: Memorie della Società Geologica Italiana, v. 45, p. 425–451.

Pauselli, C., Barchi, M.R., Federico, C., Magnani, B., and Minelli, G., 2006, The crustal structure of the Northern Apennines (central Italy): An insight by the CROP03 seismic line: American Journal of Science, v. 306, p. 428–450, doi:10.2475/06.2006.02.

Peccerillo, A., 2003, Plio-Quaternary magmatism in Italy: Episodes, v. 26, p. 222–226.

Pentecost, A., 1995, The Quaternary travertine deposits of Europe and Asia Minor: Quaternary Science Reviews, v. 14, p. 1005–1028, doi:10.1016/0277-3791(95)00101-8.

Pentecost, A., 2005, Travertine: Berlin, Springer-Verlag, 445 p.

Pentecost, A., and Viles, H., 1994, A review and reassessment of travertine classification: Géographie Physique et Quaternarie, v. 48, p. 305–314.

Piccini, L., De Waele, J., Galli, E., Polyak, V.J., Bernasconi, S.M., and Asmeromd, Y., 2015, Sulphuric acid speleogenesis and landscape evolution: Montecchio cave, Albegna River valley (southern Tuscany, Italy): Geomorphology, v. 229, p. 134–143, doi:10.1016/j.geomorph.2014.10.006.

Priewisch, A., Crossey, L.J., Karlstrom, K.E., Polyak, V.J., Asmerom, Y., Nereson, A., and Ricketts, J.W., 2014, U-series geochronology of large-volume Quaternary travertine deposits of the southeastern Colorado Plateau: Evaluating episodicity and tectonic and paleohydrologic controls: Geosphere, v. 10, no. 2, p. 401–423, doi:10.1130/GES00946.1.

Rae, A.J., Cooke, D.R., Phillips, D., Yeats, C., Ryan, C., and Hermoso, D., 2003, Spatial and temporal relationships between hydrothermal alteration assemblages at the Palinpinon geothermal field, Philippines—Implications for porphyry and epithermal ore deposits, *in* Simmons, S.F., and Graham, I., eds., Volcanic, Geothermal, and Ore-Forming Fluids: Rulers and Witnesses of Processes Within the Earth: Economic Geologists Special Publication 10, p. 223–246.

Ricketts, J.W., Karlstrom, K.E., Priewisch, A., Crossey, L.J., Polyak, V.J., and Asmerom, Y., 2014, Quaternary extension in the Rio Grande rift at elevated strain rates recorded in travertine deposits, central New Mexico: Lithosphere, v. 6, no. 1, p. 3–16, doi:10.1130/L278.1.

Rihs, S., Condomines, M., and Poidevin, J.L., 2000, Long-term behaviour of continental hydrothermal systems: U-series study of hydrothermal carbonates from the French Massif Central (Allier Valley): Geochimica et Cosmochimica Acta, v. 64, no. 18, p. 3189–3199, doi:10.1016/S0016-7037(00)00412-9.

Rimondi, V., Costagliola, P., Ruggieri, G., Benvenuti, M., Boschi, C., Brogi, A., Capezzuoli, E., Morelli, G., Gasparon, M., and Liotta, D., 2015, Investigating fossil hydrothermal systems by means of fluid inclusions and stable isotopes in banded travertine: An example from Castelnuovo dell'Abate (southern Tuscany, Italy): International Journal of Earth Sciences, v. 105, no. 2, p. 659–679, doi:10.1007/s00531-015-1186-y.

Rocchi, S., Westerman, D.S., Dini, A., Innocenti, F., and Tonarini, S., 2002, Two-stage growth of laccoliths at Elba Island, Italy: Geology, v. 30, p. 983–986, doi:10.1130/0091-7613(2002)030<0983:TSGOLA>2.0.CO;2.

Rosenbaum, G., and Lister, G.S., 2004, Neogene and Quaternary rollback evolution of the Tyrrhenian Sea, the Apennines, and the Sicilian Maghrebides: Tectonics, v. 23, p. TC1013, doi:10.1029/2003TC001518.

Rossetti, F., Tecce, F., Billi, A., and Brilli, M., 2007, Patterns of fluid flow in the contact aureole of the late Miocene Monte Capanne pluton (Elba Island, Italy): The role of structures and rheology: Contributions to Mineralogy and Petrology, v. 153, p. 743–760, doi:10.1007/s00410-006-0175-3.

Rossetti, F., Balsamo, F., Villa, I.M., Bouybaouenne, M., Faccenna, C., and Funiciello, R., 2008, Pliocene–Pleistocene HT–LP metamorphism during multiple granitic intrusions in the southern branch of the Larderello geothermal field (southern Tuscany, Italy): Journal of the Geological Society, London, v. 165, p. 247–262, doi:10.1144/0016-76492006-132.

Rossetti, F., Aldega, L., Tecce, F., Balsamo, F., Billi, A., and Brilli, M., 2011, Fluid flow within the damage zone of the Boccheggiano extensional fault (Larderello–Travale geothermal field, central Italy): Structures, alteration and implications for hydrothermal mineralization in extensional settings: Geological Magazine, v. 148, no. 4, p. 558–579, doi:10.1017/S001675681000097X.

Rowland, J.V., and Sibson, R.H., 2004, Structural controls on hydrothermal flow in a segmented rift system, Taupo volcanic zone, New Zealand: Geofluids, v. 4, p. 259–283, doi:10.1111/j.1468-8123.2004.00091.x.

Royden, L., Patacca, E., and Scandone, P., 1987, Segmentation and configuration of subducted lithosphere in Italy: An important control on thrust belt and foredeep-basins evolution: Geology, v. 15, p. 714–717, doi:10.1130/0091-7613(1987)15<714:SACOSL>2.0.CO;2.

Sella, P., Billi, A., Mazzini, I., De Filippis, L., Pizzino, L., Sciarra, A., and Quattrocchi, F., 2014, A newly-emerged (August 2013) artificially-triggered fumarole near the Fiumicino airport, Rome, Italy: Journal of Volcanology and Geothermal Research, v. 280, p. 53–66, doi:10.1016/j.jvolgeores.2014.05.008.

Serri, G., Innocenti, F., and Manetti, P., 1993, Geochemical and petrological evidence of the subduction of delaminated Adriatic continental lithosphere in the genesis of the Neogene–Quaternary magmatism in central Italy: Tectonophysics, v. 223, p. 117–147, doi:10.1016/0040-1951(93)90161-C.

Soligo, M., Tuccimei, P., Barberi, R., Delitala, M.C., Miccadei, E., and Taddeucci, A., 2002, U/Th dating of freshwater travertine from Middle Velino Valley (central Italy): Paleoclimatic and geological implications: Palaeogeography, Palaeoclimatology, Palaeoecology, v. 184, p. 147–161, doi:10.1016/S0031-0182(02)00253-5.

Sturchio, N.C., Pierce, K.L., Murrell, M.T., and Sorey, M.L., 1994, Uranium-series ages of travertines and timing of the last glaciation in the northern Yellowstone area, Wyoming–Montana: Quaternary Research, v. 41, p. 265–277, doi:10.1006/qres.1994.1030.

Taddeucci, A., and Voltaggio, M., 1987, Th-230 dating of the travertines connected to the Vulsini Mts. volcanism (northern Latium Italy): Neotectonics and hydrogeology: Periodico di Mineralogia, v. 56, p. 295–302.

Toker, E., Kayser-Özer, M.S., Özkul, M., and Kele, S., 2015, Depositional system and palaeoclimatic interpretations of middle to late Pleistocene travertines: Kocabas, Denizli, south-west Turkey: Sedimentology, v. 62, p. 1360–1383, doi:10.1111/sed.12186.
Turi, B., 1986, Stable isotope geochemistry of travertines, *in* Fritz, P., and Fontes, J.C., eds., Handbook of Environmental Isotope Geochemistry: 2. Terrestrial Environment: Amsterdam, Netherlands, Elsevier, p. 207–238.
Tzedakis, P.C., Andrieu, V., de Beaulieu, J.-L., Birks, H.J.B., Crowhurst, S., Follieri, M., Hooghiemstra, H., Magri, D., Reille, M., Sadori, L., Shackleton, N.J., and Wijmstra, T.A., 2001, Establishing a terrestrial chronological framework as a basis for biostratigraphical comparisons: Quaternary Science Reviews, v. 20, p. 1583–1592, doi:10.1016/S0277-3791(01)00025-7.
Uysal, I.T., Feng, Y., Zhao, J.X., Altunel, E., Weatherley, D., Karabacak, V., Cengiz, O., Golding, S.D., Lawrence, M.G., and Collerson, K.D., 2007, U-series dating and geochemical tracing of late Quaternary travertine in co-seismic fissures: Earth and Planetary Science Letters, v. 257, no. 3–4, p. 450–462, doi:10.1016/j.epsl.2007.03.004.
Uysal, I.T., Feng, Y., Zhao, J.X., Isik, V., Nuriel, P., and Golding, S.D., 2009, Hydrothermal CO_2 degassing in seismically active zones during the late Quaternary: Chemical Geology, v. 265, p. 442–454, doi:10.1016/j.chemgeo.2009.05.011.
van der Pluijm, B.A., and Marshak, S., 2003, Earth Structure (2nd ed.): New York, W.W. Norton & Company, 673 p.
Vignaroli, G., Aldega, L., Balsamo, F., Billi, A., De Benedetti, A.A., De Filippis, L., Giordano, G., and Rossetti, F., 2015, A way to hydrothermal paroxysm, Colli Albani volcano, Italy: Geological Society of America Bulletin, v. 127, p. 672–687, doi:10.1130/B31139.1.
Vignaroli, G., Pinton, A., De Benedetti, A.A., Giordano, G., Rossetti, F., Soligo, M., and Berardi, G., 2013, Structural compartmentalisation of a geothermal system, the Torre Alfina field (central Italy): Tectonophysics, v. 608, p. 482–498, doi:10.1016/j.tecto.2013.08.040.
Wedepohl, K., 1995, The composition of the continental crust: Geochimica et Cosmochimica Acta, v. 59, p. 1217–1232, doi:10.1016/0016-7037(95)00038-2.
Wortel, M.J.R., and Spakman, W., 2000, Subduction and slab detachment in the Mediterranean-Carpathian region: Science, v. 290, p. 1910–1917, doi:10.1126/science.290.5498.1910.
Zachos, J., Pagani, M., Sloan, L., Thomas, E., and Billups, K., 2001, Trends, rhythms, and aberrations in global climate 65 Ma to present: Science, v. 292, p. 686–693, doi:10.1126/science.1059412.
Zanchi, A., and Tozzi, M., 1987, Evoluzione paleogeografica e strutturale recente del bacino del fiume Albegna (Toscana meridionale): Geologica Romana, v. 26, p. 305–325.

MANUSCRIPT RECEIVED 16 NOVEMBER 2015
REVISED MANUSCRIPT RECEIVED 8 APRIL 2016
MANUSCRIPT ACCEPTED 19 APRIL 2016

Printed in the USA